CH3514 – Physical Chemistry and Bonding of Transition Metals

Eli Zysman-Colman (ezc)

21 Sc 44.9559 Scandium	22 Ti 47.867 Titanium	23 V 50.9415 Vanadium	24 Cr 51.9961 Chromium	25 Mn 54.938 Manganese	26 Fe 55.845 Iron	27 Co 58.9332 Cobalt	28 Ni 58.6934 Nickel	29 Cu 63.546 Copper	30 Zn 65.4089 Zinc
39 Y 88.9058 Yitrium	40 Zr 91.224 Zirconium	41 Nb 92.9064 Niobium	42 Mo 85.94 Molybdenum	43 Tc 98 Technetium	44 Ru 101.07 Ruthenium	45 Rh 102.9055 Rbodium	46 Pd 106.42 Palladium	47 Ag 107.8682 Silver	48 Cd 112.411 Cadmium
71 Lu 174.967 Lutetium	72 Hf 178.49 Hafnium	73 Ta 180.9497 Tantalum	74 W 183.84 Tungsten	75 Re 186.207 Rhenium	76 Os 190.23 Osmium	77 Ir 192.217 Iridium	78 Pt 195.084 Platinum	79 Au 196.9666 Gold	80 Hg 200.59 Mercury

1. *INTRODUCTION: Coordination Chemistry of Complexes*

This module follows from the transition metals chemistry module of CH2501. Here, there will be a focus on understanding the thermodynamics and kinetics of reactions involving metal aqua complexes. In particular, concepts relating to stepwise and global equilibrium constants and their relationship to the free energy of formation will be discussed. The chelate effect will be explored as it pertains to the thermodynamic stability of the complexes. Kinetic lability and its link to thermodynamic stability will also be investigated. Finally, there will be a more detailed exploration of both molecular orbital theory and ligand field theory.

$[Ru(bpy)_3]^{2+}$

HOMO   LUMO
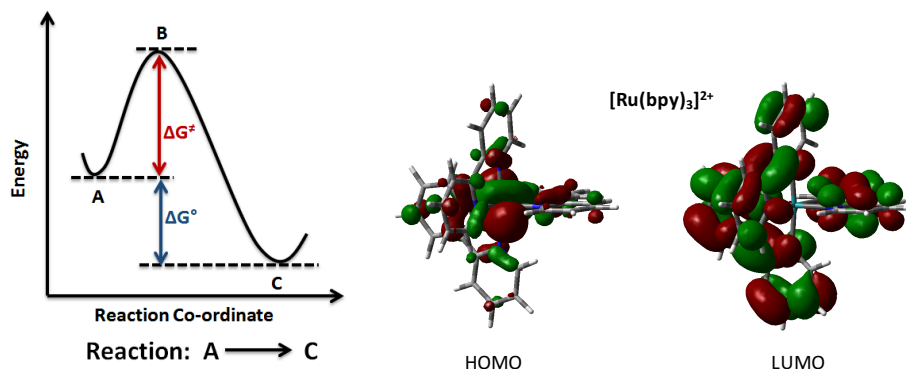
2. *MO Theory*

Before we can understand MO diagrams and bonding in complexes, we must understand the nature of the frontier MOs of ligands.

There are three types of orbital interactions between ligands and metals, which define the ligand type:
- σ-donors
- π-donors
- π-acceptors

2.1 *MO Theory: σ-Donor Ligands*
These ligands donate two e⁻s from an orbital of σ-symmetry. Examples include**:** H^-, CH_3^-, NR_3, PR_3, $OH_2.$

2.1.1 *MO Theory: σ-Donor Ligands: NH₃*
Let's look more closely at the MO diagram of NH_3 as a prototypic σ-donor. This molecule is C_3-symmetric. The symmetry adapted linear combinations (SALCs) of atomic orbitals are shown below.

3 H's

a_1

No nodes

$e^{(+)}$

$e^{(-)}$

1 node

N

$2p_z$ $2p_y$

$2s$ $2p_x$

a_1 e
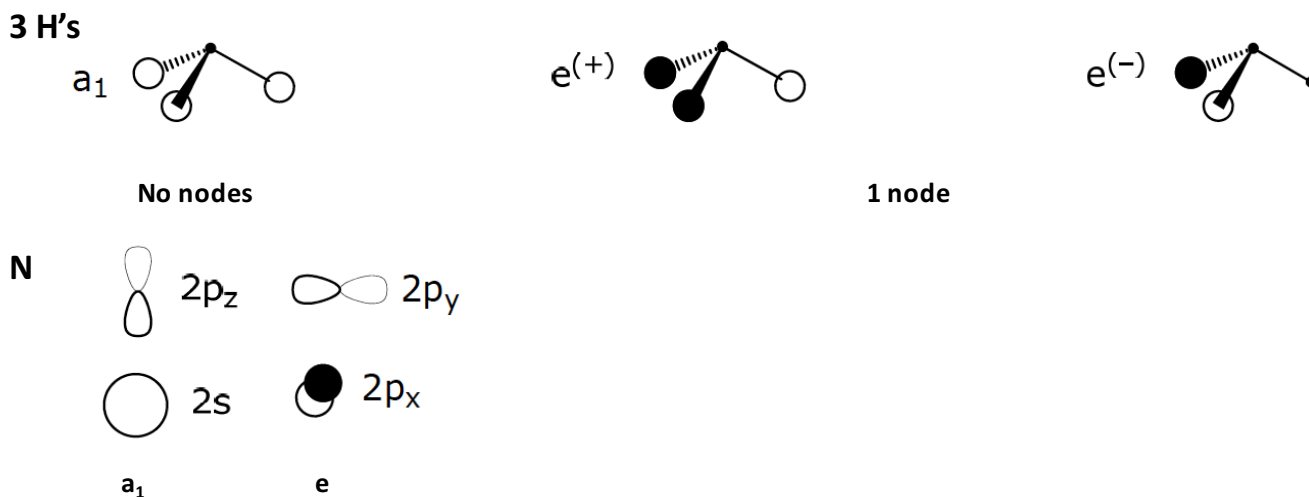
Recall that only orbitals of the same symmetry can combine to form new molecular orbitals (MOs), in what is also termed linear combinations of atomic orbitals (LCAOs). So the all in-phase SALC of a_1 symmetry can form two combinations, one with the N $2p_z$ and one with the N $2s$ orbitals. Each of the two SALCs of e symmetry (both containing one node and so higher in energy than the SALC of a_1 symmetry) can combine with one of the other two N 2p orbitals, as shown below. Notice that in each case, the phasing of the orbitals aligns (light with light and dark with dark).

a_1 $\pm$ $\left\{ \begin{array}{c} 2p_z \\ 2s \end{array} \right\}$ $\longrightarrow$ σ $\sigma*$

a_1

$e^{(+)}$ $\pm$ $2p_y$ $\xrightarrow{LCAO}$

$e^{(-)}$ $\pm$ $2p_x$ $\xrightarrow{LCAO}$ σ_b $\sigma*$

z

y

x
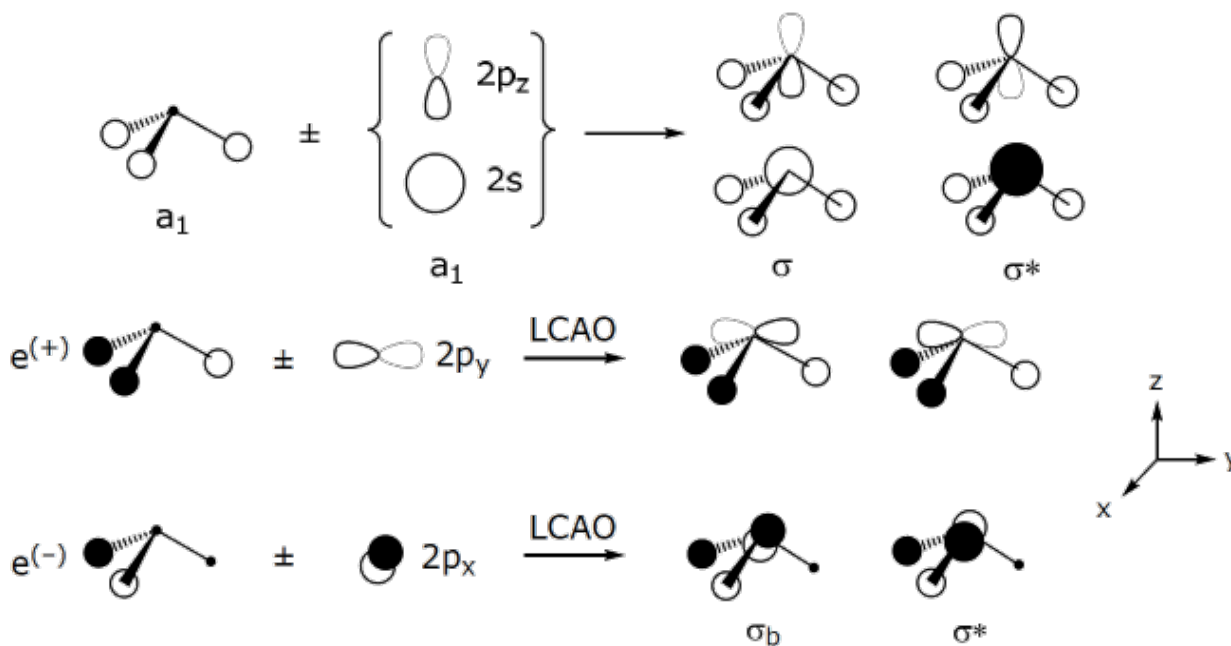
With these combinations in hand, we next need to construct the MO diagram. Remember that:
- The greater the overlap, the greater the splitting
- The closer in energy between the two sets of orbitals, the greater the splitting

Recall also that the HOMO is used for bonding to the metal and it is in this case related to the lone pair on N in a σ-orbital. The MO diagram predicts occupied MOs of three different energies, which is borne out experimentally by photoemission spectra (PES).
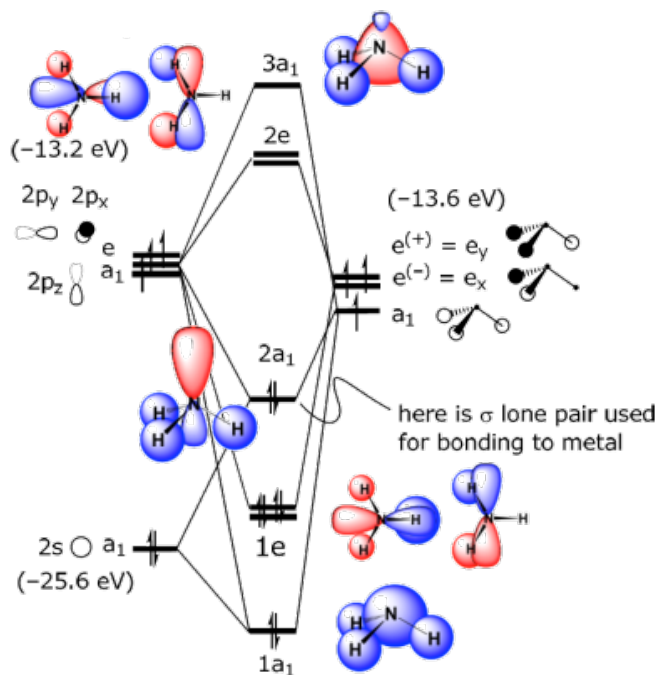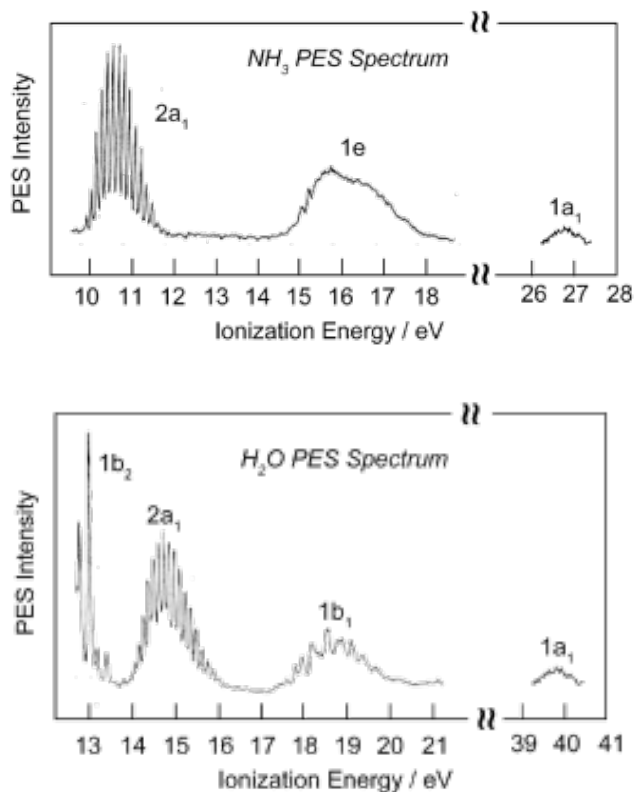
2.1.2 *MO Theory: σ-Donor Ligands: OH₂*

How do we analyse water? Recall that we saw this MO diagram in CH2501. The HOMO in water (b2) is one of the two non-bonding lone pairs on oxygen and it can bind to metals. The MO diagram predicts occupied MOs of four different energies, which is also borne out in the PES (shown above). The MO diagram is shown below left while below right one can see the SALCs of the two hydrogen atoms interacting with the central O 2s and O 2p orbitals.
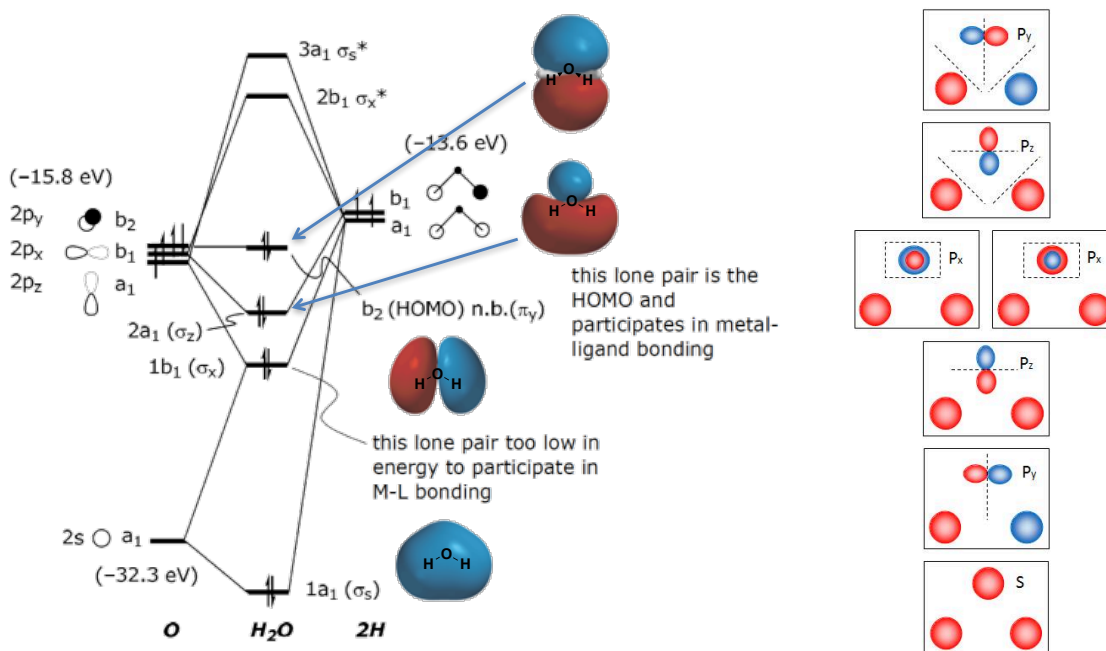
2.2 *MO Theory: π-Donor Ligands*

In addition to donating electron density to a metal via a σ-bond, e⁻s may be provided to the metal via a π-symmetry interaction.

σ-donation

and

p_z

p_y

p_x

π donation
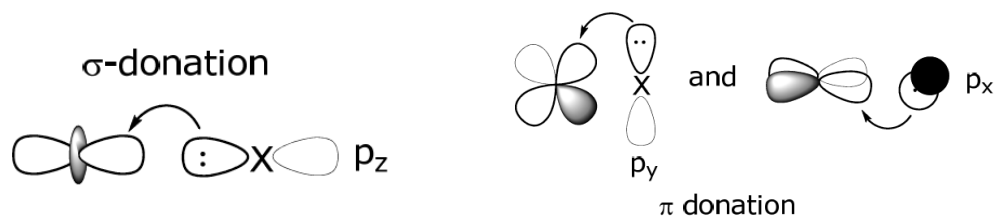
π-donor ligands include X^- (halide), amide (NR_2^-), sulfide (S^{2-}), oxide (O^{2-}), alkoxide (RO^-), η^3-C_3H_5, η^5-C_5H_5, η^6-C_6H_6. Notice that in some cases there is a lone pair in a p-orbital that is orthogonal to a first lone pair donating to the metal with σ-symmetry while in other cases, there is a π-system composed of double bonds that can donate electron density.

2.2.1 *MO Theory: π-Donor Ligands: NH$_2^-$*

Let's look at NH_2^-, which we can think of as "planar" NH_3 with a lone pair replacing one of the H atoms. This second lone pair is located in a p-orbital, oriented perpendicular to the first lone pair, which is in an sp^2-hybrid orbital. Below, left is a Walsh diagram, which shows how the MO diagram is modulated by converting the trigonal NH_3 to an all planar NH_3 molecule. One can see that in the all planar MO there is greater bonding between the N 2px and 2py orbitals with the SALCs of e symmetry. These leads to a stabilization of these orbitals. Conversely, in planarizing the structure, there is no more bonding between the N 2pz orbital and the SALC of a_1 symmetry, which leads to a destabilization of that orbital.

When analyzing NH_2^-, one of the three hydrogen atoms is replaced with a lone pair. The result here is a strong destabilization of the MO of formally e_x symmetry as we have removed a bonding interaction between the N $2p_x$ orbital and one of the three hydrogen atoms. The MO that formally was of a_2 symmetry doesn't change energy with the replacement of one of the three hydrogen atoms with the lone pair as the $2p_z$ orbital is orthogonal to the plane occupied by the lone pair.

2.3 *MO Theory: π-Acceptor Ligands*

σ-donation

π-accepting

this orbital interaction responsible for designation of these ligands as π-**acids**

This class of ligands donates e⁻s from a σ orbital and these ligands accept e⁻s from the metal into an empty π* orbital.

CO is the archetype of this ligand class. Other π-acceptors are NO^+, CN^-, CNR, H_2, C_2H_4, N_2, O_2, PR_3, BR_2.

We analyzed the MO diagram of CO in detail in CH2501. The HOMO of CO is the lone pair on carbon and this is what binds to the metal. The LUMO of CO is one of the two degenerate π* orbitals. It is into this orbital that the metal back-donates into the ligand.

2.4 *MO Theory: General Concepts*
Some important points to remember regarding MO diagrams. The M—L atomic orbital mixing between two atoms M and L is proportional to the overlap between the two atoms (S_{ML}). Owing to more directional bonding (greater overlap) along the series $S_{ML}(\sigma) > S_{ML}(\pi) > S_{ML}(\delta)$, which leads to greater splitting along the series of bonding and antibonding orbitals (therefore, σ-bonds tend to be more stabilized and the antibonding combination tends to be more destabilized than π-bonds and π-antibonding combinations). M–L atomic orbital mixing is inversely proportional to energy difference of mixing orbitals (i.e. ΔE_{ML}). So the closer in energy the two sets of orbitals, the greater the mixing (and the greater the splitting of the bonding and antibonding combinations). Only orbitals of correct symmetry can mix and the total MOs = sum of the precursor orbitals. This last point is extremely important. For most metal complexes, the order of the energies of the ligand-based and metal-based

orbitals E_L and E_M almost always is: $\sigma(L) < \pi(L) < nd < (n+1)s < (n+1)p$. The $\pi^*(L)$ can reside anywhere above the nd orbitals and the energy of the $\pi^*(L)$ orbitals is dependent on the nature of L.

Some general observations include:
- The s orbitals of the ligands (L's) are generally too low in energy to participate in bonding ($\Delta E_{ML}(\sigma)$ is very large)
- Filled p orbitals of L's are the frontier orbitals of the ligands, and they have IEs that place them below the metal orbitals
- For molecular L's, whose frontier orbitals comprise s and p orbitals, here too filled ligand orbitals have energies that are stabilized relative to the metal orbitals
- Ligand orbital energy increases with decreasing electronegativity (E_{neg}) of the Lewis basic bonding atom $E(CH_3^-) > E(NH_2^-) > E(OH^-)$
- M orbital energy decreases with increase oxidation state of metal, as you go down the periodic table and as you go from left to right on the periodic table, which is reflective in the ionization energy of the metal (see below) – recall that there is a contraction in the ionic radium across the row due to inefficient shielding of the d-orbitals by d-electrons.

Periodic table of first ionization energies (375.7 kJ/mol to 2372.3 kJ/mol):

Group	1	2	3	4	5	6	7	8	9	10	11	12	13	14	15	16	17	18
1	H 1312.0																	He 2372.3
2	Li 520.2	Be 899.5											B 800.6	C 1086.5	N 1402.3	O 1313.9	F 1681.0	Ne 2080.7
3	Na 495.8	Mg 737.7											Al 577.5	Si 786.5	P 1011.8	S 999.6	Cl 1251.2	Ar 1520.6
4	K 418.8	Ca 589.8	Sc 633.1	Ti 658.8	V 650.9	Cr 652.9	Mn 717.3	Fe 762.5	Co 760.4	Ni 737.1	Cu 745.5	Zn 906.4	Ga 578.8	Ge 762.2	As 944.5	Se 941.0	Br 1139.9	Kr 1350.8
5	Rb 403.0	Sr 549.5	2nd 1309	1414	1592	1509	1561	1644	1752	1958	Cd 867.8	In 558.3	Sn 708.6	Sb 830.6	Te 869.3	I 1008.4	Xe 1170.3	
			3rd 2650	2828	3056	3251	2956	3231	3489	3954								
6	Cs 375.7	Ba 502.9	4th 4173	4600	4900	5020	5510	5114	5404	5683	Hg 1007.1	Tl 589.4	Pb 715.6	Bi 703.0	Po 812.1	At	Rn 1037.1	
7	Fr 393.0	Ra 509.3	Ac 498.8	Rf 580	Db	Sg	Bh	Hs	Mt	Ds	Rg	Uub	Uut	Uuq	Uup			

Lanthanides 6	Ce 534.4	Pr 528.1	Nd 533.1	Pm 538.6	Sm 544.5	Eu 547.1	Gd 593.4	Tb 565.8	Dy 573.0	Ho 581.0	Er 589.3	Tm 596.7	Yb 603.4	Lu 523.5
Actinides 7	Th 608.5	Pa 568	U 597.6	Np 604.5	Pu 581.4	Am 576.4	Cm 578.1	Bk 598.0	Cf 606.1	Es 619	Fm 627	Md 635	No 642	Lr 472.8

3 LIGAND FIELD THEORY (LFT), REVISITED.

Now that we have investigated the MO diagrams of the ligands, let us now try and understand in more detail LFT, which is the interaction of ligand MOs with metal AOs.

What is LFT?

LFT is a more complete theory of bonding within complexes, and incorporates aspects of crystal field theory with MO theory. Ligand field theory attempts to incorporate the overlap of metal-based d orbitals with ligand orbitals of suitable symmetry. This approach tries to explain, among other things, the effect of different ligands on Δ_o.

LFT analyses bonding of metal s, p and d orbitals with SALCs of the ligands, which are usually formed of s and p orbitals. There are two principal bonding bonds, similar to what we have seen previously. They are σ- and π-bonding. New bonding between two metals can also have δ-symmetry (see CH2501 notes).

3.1 *LIGAND FIELD THEORY (LFT), REVISITED – Octahedral Complexes.*

Sigma (σ) bonding
- Neutral ligands (e.g., NH_3) or anionic ligands (e.g., F^-) possess lone pairs that can bond to metal-based orbitals (s, p_x, p_y, p_z, d_{xy}, d_{yz}, d_{xz}, d_{x2-y2}, d_{z2}) with σ-symmetry
- In an O_h complex, 6 SALCs of the 6 ligand σ-symmetry orbitals can be formed
- MOs for the resulting complex are formed by combining the ligand SALCs and the metal-based d-orbitals of the same symmetry type (which will be of e_g symmetry)
- With 6 SALCs combined with the metal MOs, we will get 6 bonding and 6 antibonding MOs – now called **ligand group orbitals (LGOs)**
- The resulting MO diagram now gets populated with the electrons according to the Aufbau process, Pauli exclusion principle and Hund's rule
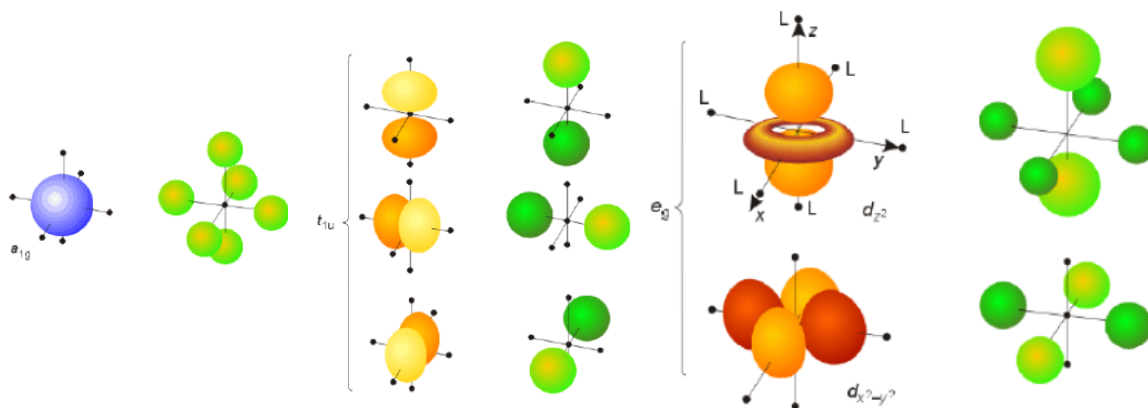
Above you can see the different SALCs interacting with the metal s (left), p (middle) and d (right) orbitals. For the Ligand SALCs, these are composed uniquely of s orbitals for the sake of simplicity above

but are shown as sp³ hybrid orbitals below. The d_{xy}, d_{xz} and d_{yz} orbitals do not have the appropriate symmetry to combine to form new LGOs. In addition, the ligand SALCS can interact with the metal s and p orbitals.
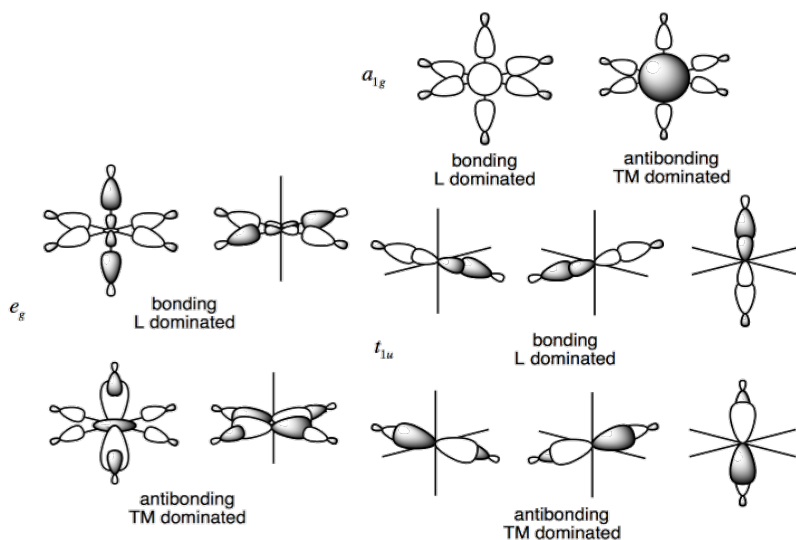
If we now look at the corresponding MO diagram (below), we see that the new bonding/antibonding MO combination of the d_{x2-y2} and d_{z2} orbitals are now called e_g and e_g*, respectively. The e_g MO is very ligand based (it is closer in energy to the ligand SALCs) while the e_g* is more metal based. The three d orbitals constituting the t_{2g} set are now non-bonding. Notice that the d-orbital splitting pattern is exactly the

same as was observed in CFT with an energy difference of Δ_o. The MO diagram below represents $[Co(NH_3)_6]^{3+}$.
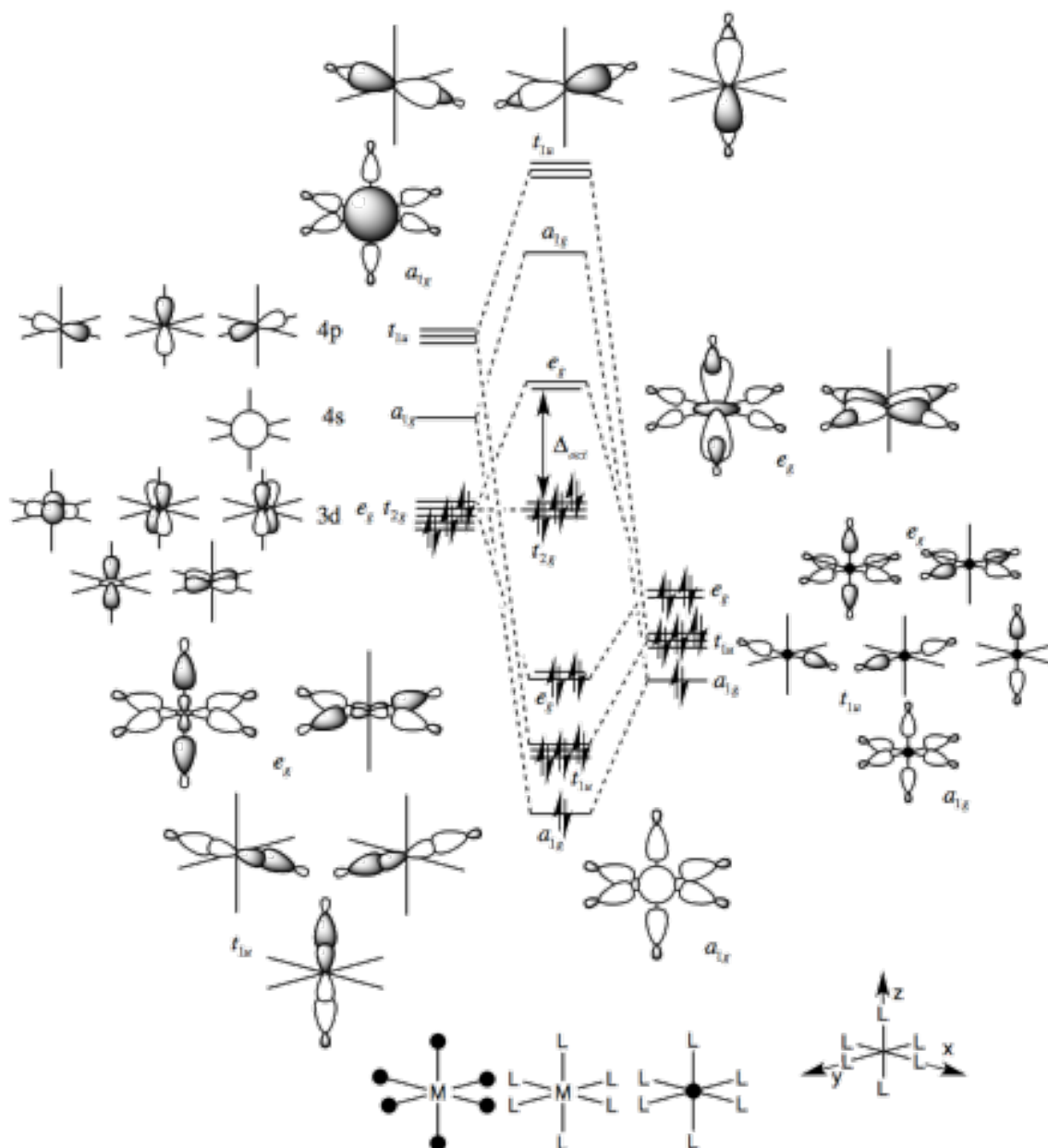
Pi (π) bonding:

The previous MO diagram ignores π bonding. If the ligands possess orbitals of local π-symmetry then these can interact with the metal d-orbitals with the same symmetry (i.e. the t_{2g} set in an octahedral complex) to form new LGOs in addition to all the LGOs we have just discussed that have σ-symmetry. These ligand SALCs can act as electron donors (populated) or electron acceptors (vacant). We know these as π-donor and π-acceptor ligands, respectively. The nature of this secondary interaction will affect Δ_o.
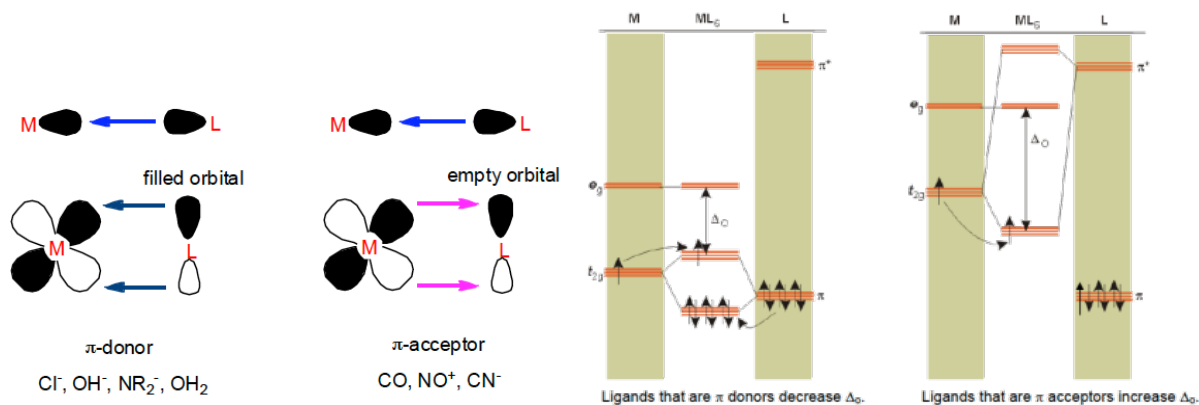
If the π-bond that is formed is composed of unoccupied d-orbitals with occupied p-orbitals on the ligands, then this is the case of π-**donor ligands (π-bases)**. Above left is an MO diagram demonstrating the impact of the new bonding/antibonding combination of the ligand SALCs interacting with the metal t_{2g} set. The impact of this new interaction is to destabilize the antibonding t_{2g}^* orbital that contains large metal character, thereby decreasing Δ_o. The corresponding ligand-based t_{2g} orbitals are stabilized. 3-d Metal complexes with π-donor ligands are frequently high spin due to the smaller Δ_o. An example of such a complex is $[FeCl_6]^{3-}$. Below left is the complete MO diagram for an octahedral complex with π-donor ligands.
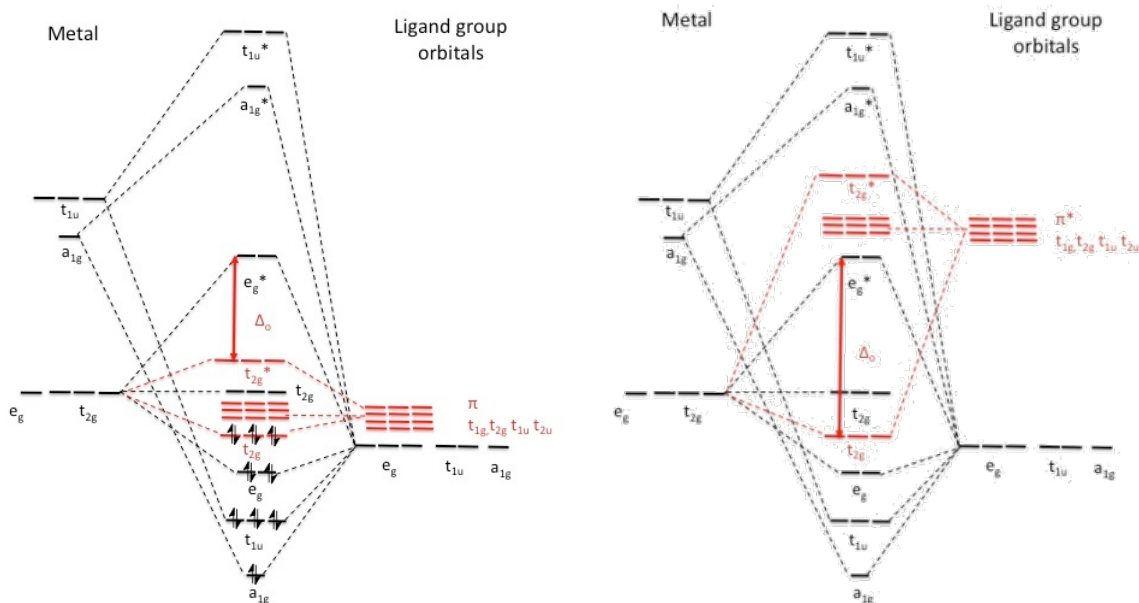
If the π-bond that is formed is composed of occupied d-orbitals with unoccupied p-orbitals on the ligands, then this is the case of π-**acceptor ligands (π-acids)**. Above right is an MO diagram demonstrating the impact of the new bonding/antibonding combination of the ligand SALCs interacting with the metal t_{2g} set. The impact of this new interaction is to stabilize the bonding t_{2g} orbital that contains large metal character, thereby increasing Δ_o. The corresponding t_{2g} orbitals containing large degrees of ligand character are now destabilized (t_{2g}^*). Recall that Δ_o refers only to the energy difference between the metal-based MOs. The interaction of the metal t_{2g} orbitals with π-acceptor ligands is frequently called π-**backbonding**. π-Backbonding effectively removes electron density from the metal, which does not like to have too high an electron density. Complexes with π-acceptor ligands are frequently low spin due to the larger Δ_o. An example of such a complex is $[Cr(CO)_6]$. The full MO diagram is on the right in the lower figure above.

Take home message: π-bonding and π-backbonding modulate the energy of the metal t_{2g} orbitals. This secondary bonding interaction now explains the spectrochemical series.

$$I^- < S^{2-} < F^- < OH^- < H_2O < NH_3 < NO_2^- < CN^- < CO \sim NO < NO^+$$
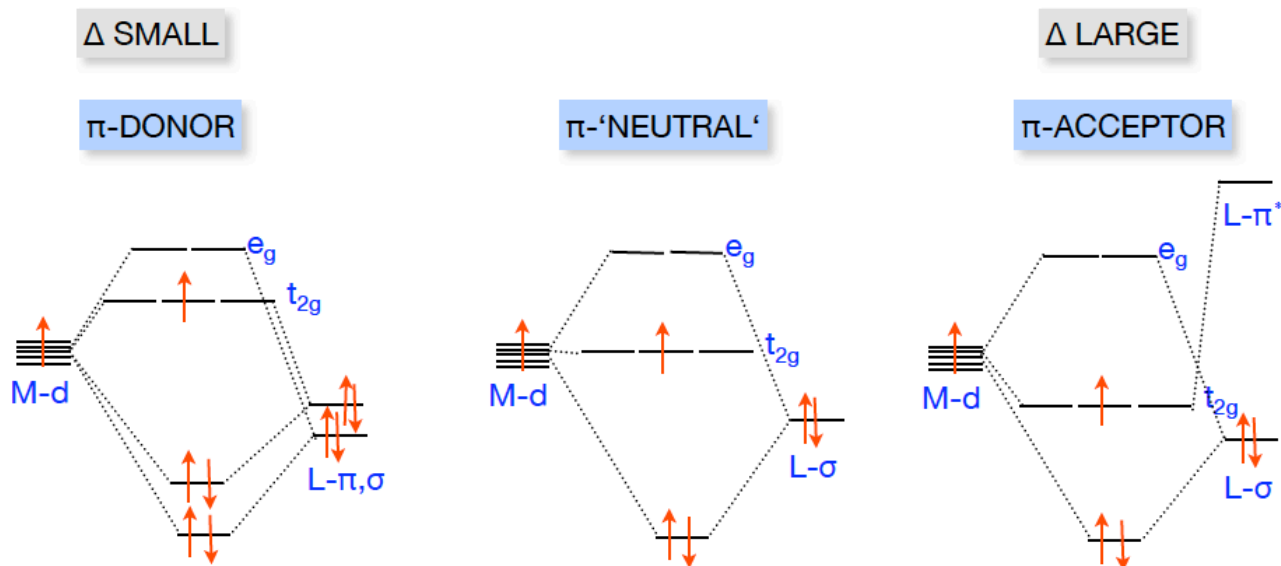
3.2 *LIGAND FIELD THEORY (LFT), REVISITED – Square Planar Complexes.*

How do we apply LFT to complexes with other geometries? We apply the same principles as we did for octahedral complexes. Let's look at square planar complexes, which we can think of as octahedral complexes without the two axial ligands. Let's use $[Pd(NH_3)_4]^{2+}$ as the example, where the ligand shows only sigma donation. The resulting MO diagram should therefore mirror, for the d-orbital splitting, the same pattern as CFT.
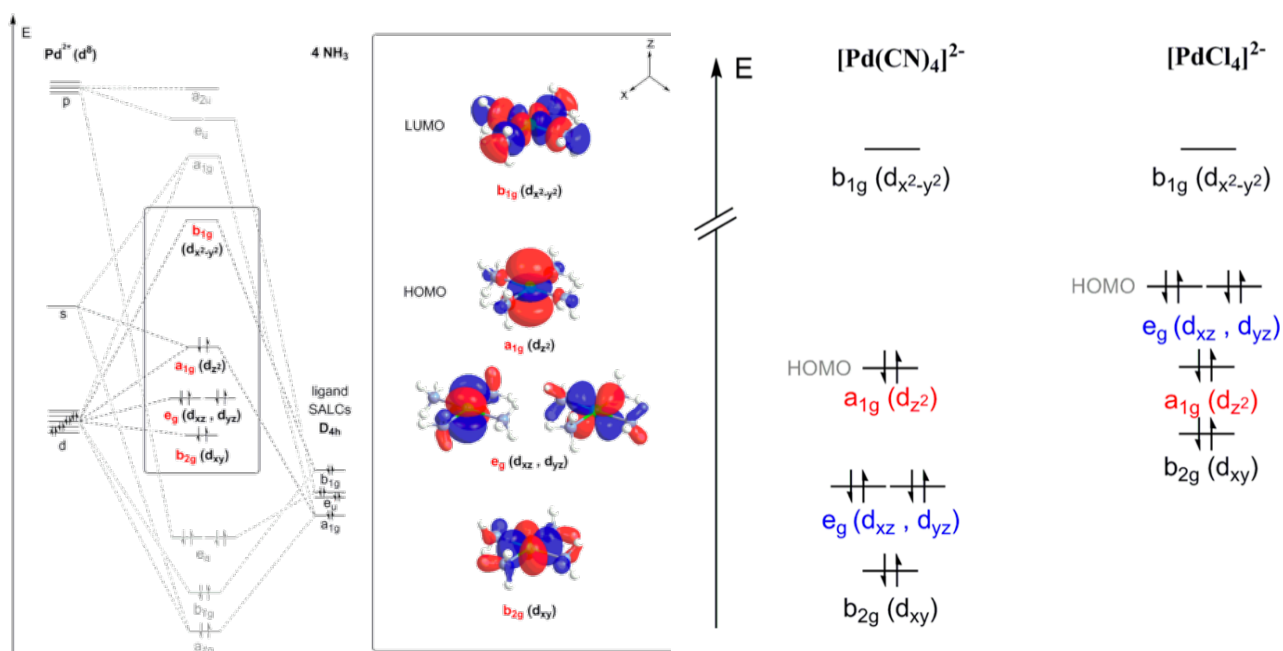
We can now see in the left-hand figure above that the d_{x2-y2} MO (b_{1g}) contains very strong metal–ligand antibonding interactions in the xy plane. It is the **LUMO**. There is a corresponding stabilized b_{1g} orbital that has a strong ligand character. The d_{z2} MO (a_{1g}) contains slight metal–ligand antibonding interactions in the xy plane due to the donut part of the d_{z2} orbital. It is the **HOMO**. Contrast these two orbitals with the e_g* set in the octahedral case where both the d_{x2-y2} and d_{z2} orbitals interacted equally with the ligand SALCS and so were equally destabilized in the new LGOs. In the square planar complex, this is not the case. The d_{xy}, d_{xz}, d_{yz}, MO (e_g, b_{2g}) are normally presented as degenerate and non-bonding (no symmetry match with ligand MOs). The observed splitting of these orbitals into two sets (e_g and b_{2g}) is required by group theory considerations according to the irreducible representations of the D_{4h} point group, and is beyond the scope of this course.

What about ligands with π-character? Including π-interactions results in a re-ordering of the energies of the MOs, unlike what we saw with O_h complexes. For complexes with π-donating ligands, such as $[PdCl_4]^{2-}$, the HOMO is the e_g MOs (d_{xz} and d_{yz}) and not the a_{1g} MO as a result of the destabilization from π-antibonding interactions with the lone pairs of the ligands. In addition, the a_{1g} MO is energetically stabilized, due to the weak σ-donating properties of ligands interacting with the metal d_{z2} orbital. For π-accepting ligands, such as $[Pd(CN)_4]^{2-}$, the order of the LGOs remains the same but the e_g set containing mainly metal character is stabilized.

4 WATER AS A LIGAND IN 3-d METAL COMPLEXES.

Since water can be viewed as the most fundamental ligand, we will use aqueous solutions and the species found therein as the basis for exploring the chemistry of 3-d metal complexes. The table below details the various metal aqua complexes that exist as a function of metal identity and oxidation state.

	II	III	IV	V	VI	VII
Sc	-	$[Sc(OH_2)_7]^{3+}$ d^0				
Ti	$[Ti(OH_2)_6]^{2+}$ d^2	$[Ti(OH_2)_6]^{3+}$ d^1				
V	$[V(OH_2)_6]^{2+}$ d^3	$[V(OH_2)_6]^{3+}$ d^2	$[VO(OH_2)_5]^{2+}$ d^1	$[VO_2(OH_2)_4]^{+}$ $[VO_4]^{3-}$ d^0		
Cr	$[Cr(OH_2)_6]^{2+}$ d^4	$[Cr(OH_2)_6]^{3+}$ d^3	$[CrO(OH_2)_5]^{2+}$ d^2		$[Cr_2O_7]^{2-}$ $[CrO_4]^{2-}$ d^0	
Mn	$[Mn(OH_2)_6]^{2+}$	$[Mn(OH_2)_6]^{3+}$	-	$[MnO_4]^{3-}$	$[MnO_4]^{2-}$	$[MnO_4]^{-}$

	d^5	d^4		d^2	d^1	d^0
Fe	$[Fe(OH_2)_6]^{2+}$ d^6	$[Fe(OH_2)_6]^{3+}$ d^5	$[FeO(OH_2)_5]^{2+}$ d^4		$[FeO_4]^{2-}$ d^2	
Co	$[Co(OH_2)_6]^{2+}$ d^7	$[Co(OH_2)_6]^{3+}$ d^6	-			
Ni	$[Ni(OH_2)_6]^{2+}$ d^8	-	-			
Cu	$[Cu(OH_2)_n]^{2+}$ d^9 (n = 5 or 6)	-	-			
Zn	$[Zn(OH_2)_6]^{2+}$ d^{10}	-	-			

Those complexes in green are thermodynamically stable. Those in purple are metastable. Those in red are reducing (i.e. hydrogen is generated through water decomposition) and those in blue are oxidizing (i.e. oxygen is generated through water decomposition).

Depending on the oxidation state and identity of the metal, the water ligand can either exists as a neutral H_2O ligand, M-OH_2, as an anionic deprotonated OH^- ligand, M-OH, or as a doubly deprotonated oxo ligand, M=O. The most common geometries are octahedral and tetrahedral and this depends both on the identity of the metal and also on the oxidation state.

Depending on the kinetic lability of the ligands (more on this concept later), 5-coordinate complexes are also possible, though unusual. This is the case with Cu^{2+}, which shows Jahn-Teller distortion

Cu²⁺ d⁹
rapid interconversion between 5 and 6 coordination

tetragonal - Jahn-Teller distortion square pyramidal trigonal bipyramidal
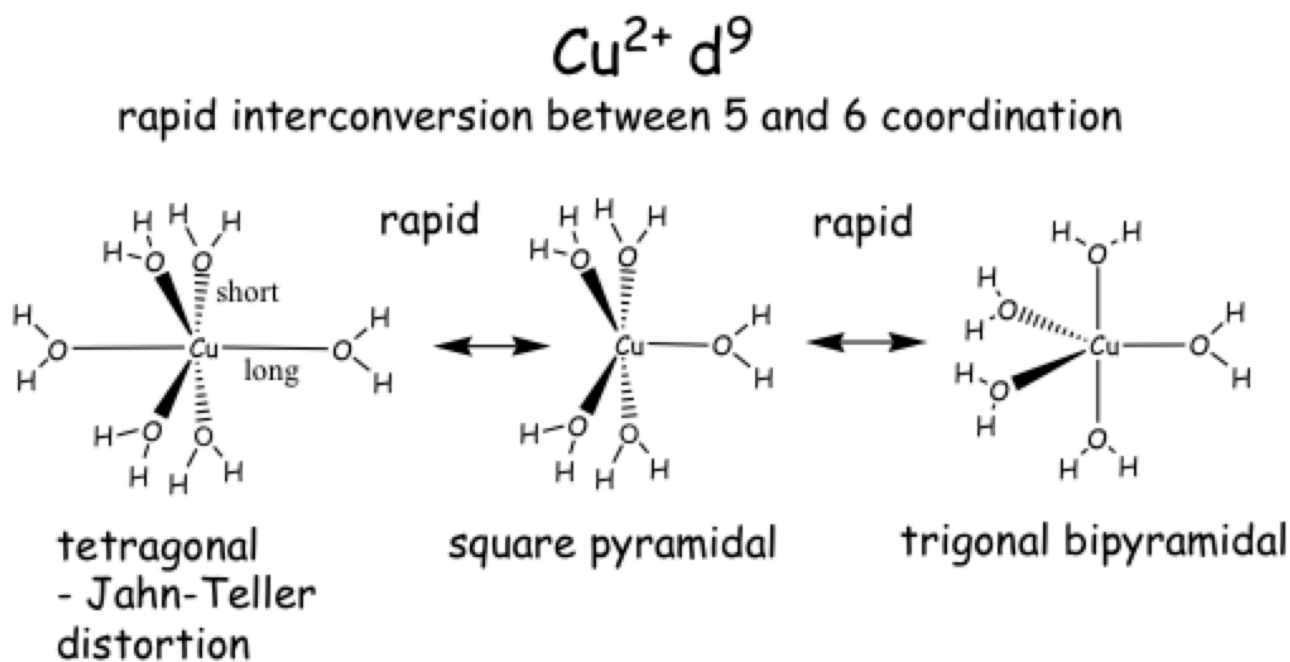
Scandium(III) is d^0 and so is a particularly large ion and it can accommodate 7 water molecules to adopt a pentagonal bipyramidal geometry.

$[Mn(OH_2)_6]^{2+}$ as an example is octahedral while $[MnO_4]^-$ is tetrahedral, the result of the much smaller Mn^{7+} ion. Why are the water ligands deprotonated so much in permanganate? The clue lies in the acid-base chemistry of these complexes.
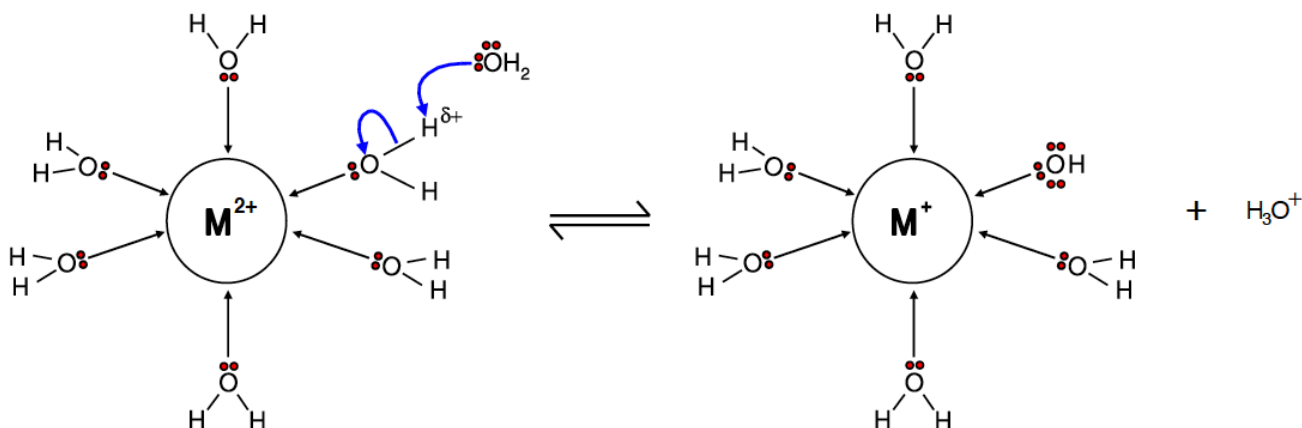
The metal acts as a Lewis Acid (LA). When H_2O complexes to the metal, the O-H bond is polarized and the proton becomes acidic and so can be abstracted by solvent water molecules. As the charge density increases on the metal (i.e. higher oxidation state of the metal), the O-H bond becomes more polarized and the proton acidity increases and more protons are abstracted into solution and the OH_2 ligand becomes an OH^- ligand, **reducing the overall charge of the complex**. The water solution thus becomes **more acidic as well**. In certain cases, the metal becomes so Lewis acidic that a second proton can be abstracted by the water solvent molecules and the OH^- can become O^{2-}. Oxo groups possess other traits that help to stabilize the resulting metal complex. They take up less space than 2 OH^-, which is important because the high oxidation state metal centres are very small. O^{2-} helps to neutralize high charge on the metal from high OS due to its higher negative charge. For metals with low d-electron count, strong π-donor ability helps to stabilize t_{2g} orbital.

Therefore, a set of equilibria reactions exists as shown below. The equilibrium can be modulated. Addition of base will shift the equilibrium to the right while addition of acid will favour an equilibrium to the left.

$$[M(H_2O)_6]^{2+}(aq) \rightleftharpoons [M(OH)(H_2O)_5]^+(aq) \rightleftharpoons [M(OH)_2(H_2O)_4](s) \rightleftharpoons$$

$$[M(OH)_3(H_2O)_3]^-_{(aq)}(aq) \rightleftharpoons [M(OH)_4(H_2O)_2]^{2-}(aq) \rightleftharpoons M(OH)_5(H_2O)]^{3-}(aq)$$

$$\rightleftharpoons [M(OH)_6]^{4-}(aq)$$
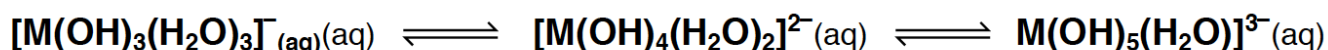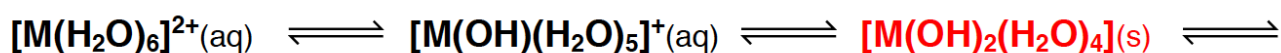
We can determine the relative acidities of $[M(OH_2)_6]^{2+}$ and $[M(OH_2)_6]^{3+}$ ions in terms of the respective pKa values.

$$[M(OH_2)_6]^{n+} + H_2O \xrightleftharpoons{K_a} [M(OH_2)_5OH]^{(n-1)+} + H_3O^+$$
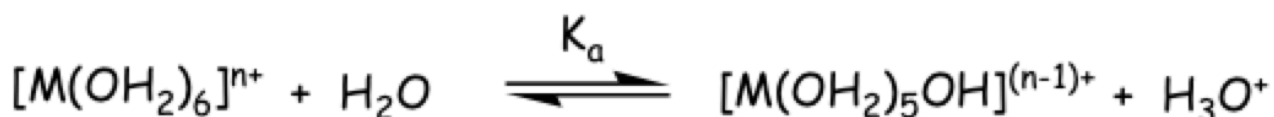
$$K_a = \frac{[M(OH_2)_5OH^{(n-1)+}][H_3O^+]}{[M(OH_2)_6{}^{n+}]} \qquad pK_a = -\log_{10} K_a$$

$$Fe^{2+} \qquad pK_a = 9.5$$
$$Fe^{3+} \qquad pK_a = 2.2$$

We can see that the pK_a for $[Fe(OH_2)_6]^{3+}$ is similar to that of formic acid (2.0) and this Lewis acid is acidic enough to react with carbonate to liberate CO_2. We can also see that as the oxidation state increases, the pKa decreases quite dramatically.

Understanding this more generally, we can associate a pKa of a particular ion with an electrostatic parameter, ξ, which is equal to Z^2/r, where Z is the atomic number and r is the ionic radius. The pKa can be derived from the pH of the water and the oxidation state of the metal by:

$$pK_a = pH - \log_{10}\frac{[M^{(n-1)+}]}{[M^{n+}]}$$

or can be empirically derived from the electronegativity of the metal by:

$$pK_a = 15.14 - 0.8816\left\{\frac{Z^2}{r} + 9.60(\chi_{Pauling} - 1.50)\right\}$$
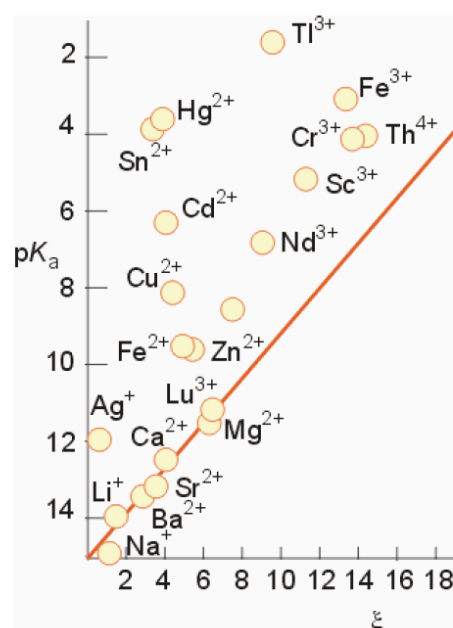
Aside from the deprotonation chemistry discussed above, substitution chemistry is also possible between two adjacent complexes, resulting in the formation of μ-OH⁻-bridged metal dimer species. This process is called "olation"
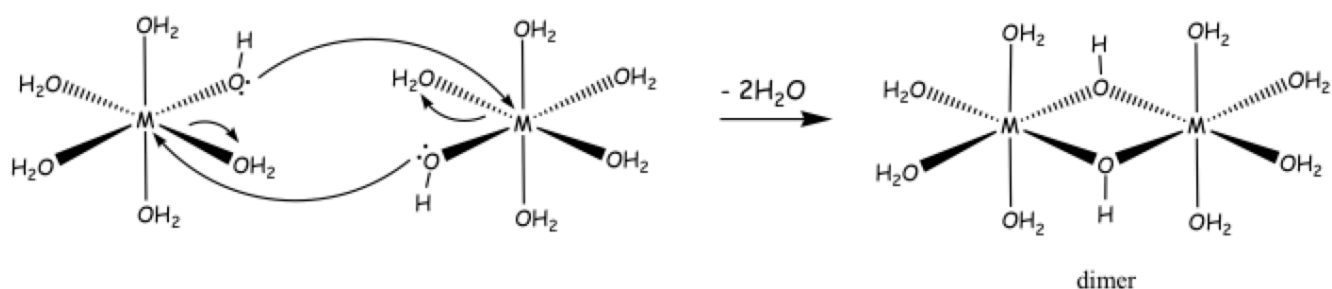
This process can continue - building up huge OH⁻ bridged polynuclear structures until solubility limits are exceeded resulting in precipitation of the hydroxide; $M(OH)_3$ aq. Accompanying dehydration can also occur leading to oxy-hydroxide or oxide (M_2O_3) forms precipitating. Fe(III) hydrolysis has been well studied and polymeric nanostructures containing over 100 iron atoms have been characterized before $Fe(OH)_3$ precipitation. The formation of oxo bridges is "oxolation".

4.1 *Fe HYDROLYSIS IN VIVO.*
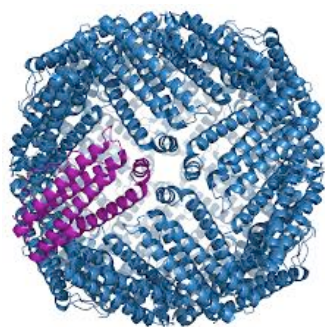
Ferritin (left) is a protein that stores iron in our body by concentrating it *via* controlled hydrolysis of Fe^{3+} aq to yield huge oxy-hydroxy bridged nanostructures containing up to 4500 iron atoms. Movement of iron in and out of the protein is achieved via reduction to Fe^{2+}_{aq}, which does not hydrolyse at pH 7 and passes through specific M^{2+}-sensing channels.

The instability of Fe^{3+} aq solutions at pH 7 with respect to hydrolysis to insoluble $Fe(OH)_3$ makes it a challenge for biology to concentrate iron in the body. Note the solubility product equilibrium constant that is very very small, ($K_{sp} = 2.6 \times 10^{-39}$).

To circumvent this issue Nature has evolved very powerful agents that bind and solubilize all forms of Fe(III) even $Fe(OH)_3$ to enable efficient iron uptake. These compounds are called **siderophores** *(Greek-iron carrier).* Some of these have the highest measured equilibrium constants for a metal ion - ligand combination. The record value is held by enterobactin. The catecholate (dihydroxybenzene) fragments chelate the iron very strongly as shown schematically below. Catecholate binding isn't the only motif used to coordinate iron. Hydroxamate-based siderophores also exist.
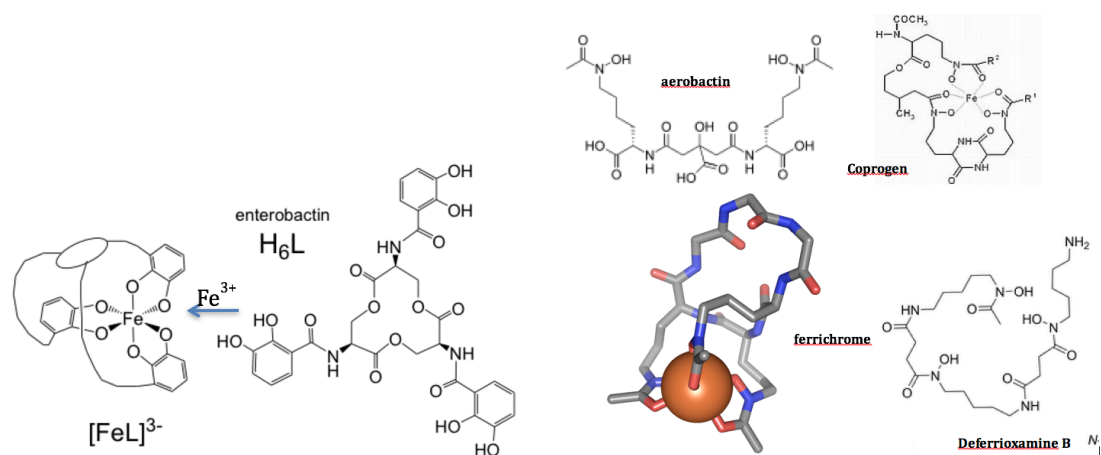
The table below documents equilibrium constants for the siderophores shown above.

siderophore	donor set	log K
aerobactin	hydroxamate, carboxylate	22.5
coprogen	hydroxamate	30.2
deferrioxamine B	hydroxamate	30.5
ferrichrome	hydroxamate	32.0
Enterobactin	catecholate	49.0

4.2 A CLOSER LOOK AT THE HYDROLYSIS REACTION.

Let's look at ligand exchange in more detail by looking at:
$[M(OH_2)_6]^{n+} + mL \rightarrow [M(OH_2)_{6-m}mL]^{n+} \rightarrow\rightarrow [M(L)_6]^{n+}$ (L is a neutral ligand).
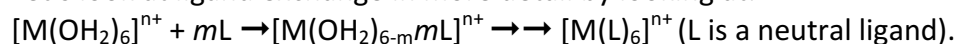
From this multiple ligand exchange reaction, we can derive stepwise equilibrium constants, K_1-K_6.

$$[M(OH_2)_6]^{n+} + L \overset{K_1}{\rightleftharpoons} [M(OH_2)_5L]^{n+} + H_2O \qquad K_1 = \frac{[M(OH_2)_5L^{n+}]}{[M(OH_2)_6^{n+}][L]}$$

$$[M(OH_2)_5L]^{n+} + L \overset{K_2}{\rightleftharpoons} [M(OH_2)_4L_2]^{n+} + H_2O \qquad K_2 = \frac{[M(OH_2)_4L_2^{n+}]}{[M(OH_2)_5L^{n+}][L]}$$

$$[M(OH_2)L_5]^{n+} + L \overset{K_6}{\rightleftharpoons} [ML_6]^{n+} + H_2O \qquad K_6 = \frac{[ML_6^{n+}]}{[M(OH_2)L_5^{n+}][L]}$$
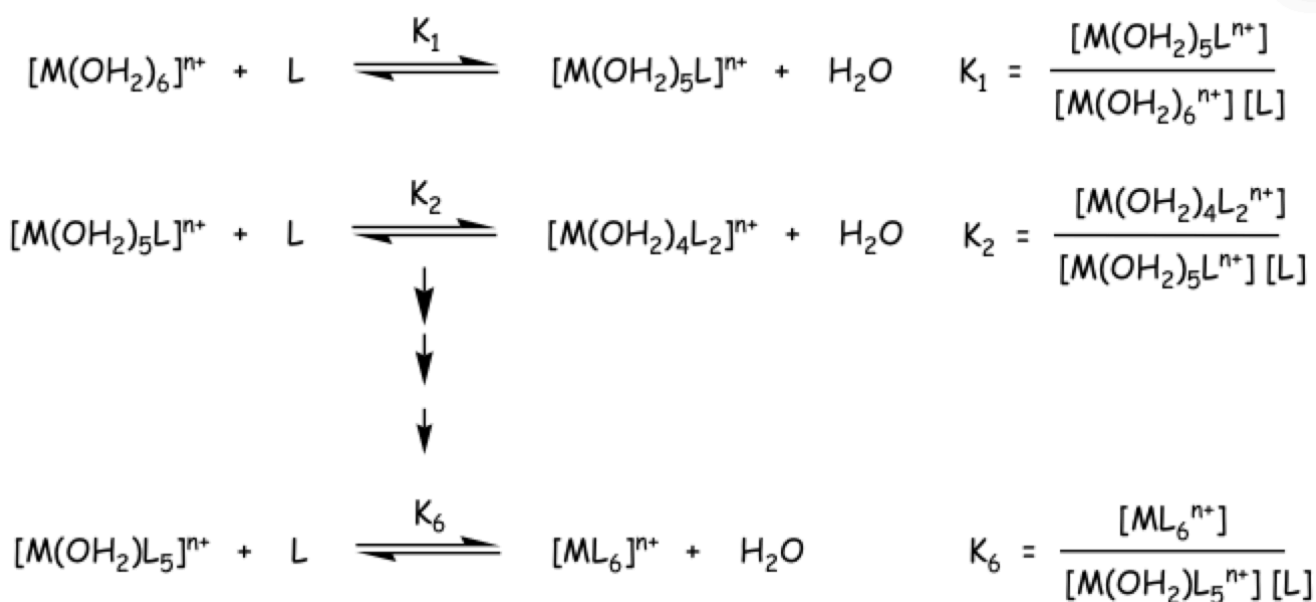
We can now define an overall stability constant, β_n for the complete exchange of H_2O ligands for L.

$$[M(OH_2)_6]^{n+} + 6L \xrightarrow{\beta_6} [ML_6]^{n+} + 6\,H_2O \qquad \beta_6 = \frac{[ML_6^{n+}]}{[M(OH_2)_6^{n+}]\,[L]^6}$$
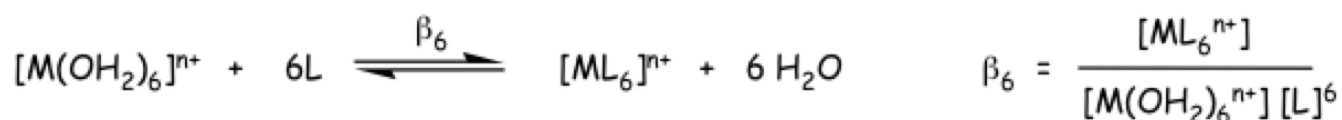
So $\beta_6 = K_1{}^*K_2{}^*K_3{}^*K_4{}^*K_5{}^*K_6$ and $\log(\beta_6) = \log(K_1) + \log(K_2) + \log(K_3) + \log(K_4) + \log(K_5) + \log(K_6)$.

What this implies is that $\beta_6 > \beta_5 > \beta_4 > \beta_3 > \beta_2 > \beta_1$ and so there will always be complete substitution of L for H_2O if the incoming ligand binds more strongly to the metal than water.

An example: NH_3 replacing H_2O on $[Ni(OH_2)_6]^{2+}$ with stepwise equilibrium constants shown below. Note the steady fall in K_n. What this data means is that $[Ni(OH_2)_6]^{2+}$ + excess NH_3 gives only $[Ni(NH_3)_6]^{2+}$.

Log β_6 = 2.79 + 2.26 + 1.69 + 1.25 + 0.74 + 0.03 = 8.76
β_6 = 5.75 x 10^8

-Log K_1	-Log K_2	-Log K_3	-Log K_4	-Log K_5	-Log K_6
-2.79	-2.26	-1.69	-1.25	-0.74	-0.03

With known equilibrium constants, K_n, we can determine free energy ΔG_n.

ΔG_n = -RT ln(K_n), where R is the gas constant 8.314 J mol^{-1} K^{-1}
So at 303 K, ΔG_1 = -(8.314 x 10^{-3} * 303) ln($10^{2.79}$) = **-16.2 kJ mol^{-1}**

$\Delta G_n = \Delta H_n - T\Delta S_n$
If ΔH_1 = **-16.8 kJ mol^{-1}**
$\Delta S_1 = (\Delta H_1 - \Delta G_1)/T = [-16.8 - (-16.2)]/303 =$ **-1.98 J mol^{-1} K^{-1}**.

One can see that the entropic term is negligible. Therefore, substitution is primarily an **enthalpic effect** (ΔH is governing the process). This is due to the stronger Ni^{2+}-N bonds being formed compared to the Ni^{2+}-O bonds (more exothermic).

5 *HARD-SOFT ACID BASE THEORY.*

HSAB Theory is a concept that is used to rationalize the stability of certain interactions between atoms. 'Hard' applies to species that are small, have high charge states and are either very electropositive or very electronegative (orange elements below), and are weakly polarizable. 'Soft' applies to species that are big, have low charge states and are strongly polarizable (blue elements below).

The total energy of an interaction, as defined by the Salem-Klopman equation, is governed by several terms, including an electrostatic term (second term) and a molecular overlap term (third term).

Salem-Klopman Equation (simplified)

$$\Delta E = - \underbrace{\frac{Q_{nuc}Q_{elec}}{\varepsilon R}}_{\text{second term}} + \underbrace{\frac{2(c_{nuc}c_{elec}\beta)^2}{E_{HOMO} - E_{LUMO}}}_{\text{third term}}$$

Thus, Hard-Hard (HH) interactions, which maximize the electrostatic interactions or Soft-Soft (SS) interactions, which maximize the molecular orbital interaction, provide more stable compounds. Hard-Soft interactions generate weaker interactions between the two atoms in the bond.

The golden rule: The Strongest M-L interactions require HH or SS match

Consider the following data on equilibrium constants for the reaction to the left.

$$Fe^{3+}_{aq} + X^- \underset{}{\overset{K_1}{\rightleftharpoons}} FeX^{2+}_{aq} + H_2O$$

$$Hg^{2+}_{aq} + X^- \rightleftharpoons HgX^{2+}_{aq} + H_2O$$
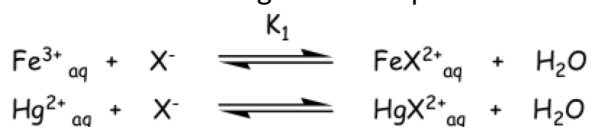
Metal Ion	$\log_{10}K_1$			
	X = F	X = Cl	X = Br	X = I
Fe^{3+}_{aq}	6.0	1.4	0.5	
Hg^{2+}_{aq}	1.0	6.7	8.9	12.9

The halides get harder as the size gets smaller.

The behaviour of Fe^{3+}_{aq} is paralleled by similar behaviour shown by the Group 1 and 2 metals and the early 3d transition elements to the left of the periodic table.

The behaviour of Hg^{2+}_{aq} is paralleled by similar behaviour shown by the heavier p–block elements and the heavier transition elements to the right of the periodic table.

General trends are:

Order of increasing stability in complexes for **Hard** metal ions: O >> S > Se > Te

N >> P > As > Sb

Order of increasing stability in complexes for **Soft** metal ions: O << S > Se ~ Te

N << P > As > Sb

Order of decreasing hardness based on electronegativity: F > O > N > Cl > Br > C ~ I ~ S > Se > P > As > Sb

Ligands displace water in a competitive process that is at equilibrium (so under thermodynamic control). If the M^{n+} is a **hard** metal - it is already associated with **hard H_2O** ligands. Thus, reaction with another hard ligand may not be favourable – only a small exothermic enthalpy effect might be seen.

Leads only to moderately stable complexes (-ΔG^o small)
        e.g., with L = RCO_2^-, F^-, Cl^- etc.

Now if M^{n+} is a **soft metal** and **L** is a **soft base** the reaction is now highly favoured since it removes two unfavourable soft-hard interactions - from water solvation.
Here a significant ΔH^o effect (large and negative) is seen when the soft-soft interaction results - leads to stable complexes with ΔG^o that is also large and negative (ΔS^o small as before) - high K_n
        e.g., Hg^{2+}_{aq} and $S^{2-}_{aq} \rightarrow HgS(s)$ precipitates

6 THE IRVING-WILLIAMS SERIES.

We have previously examined the values of log K_n (β_n) for the successive replacement of H_2O on Ni^{2+}_{aq} by NH_3
What happens along the 3d series from Sc – Zn? The figure below shows the equilibrium constant for the first substitution of NH_3 for H_2O. This trend showing a maximum in log K_1 values for Cu^{2+} is termed **the Irving-Williams series**

Values of $log_{10} K_1$ for NH_3 replacing water on $[M(OH_2)_6]^{2+}$
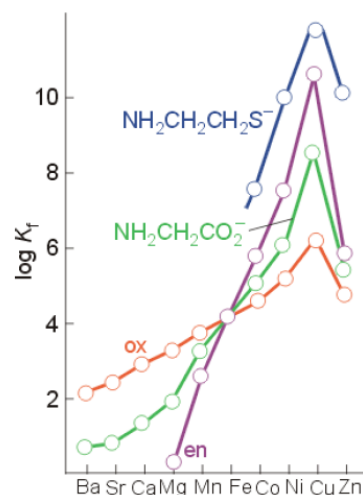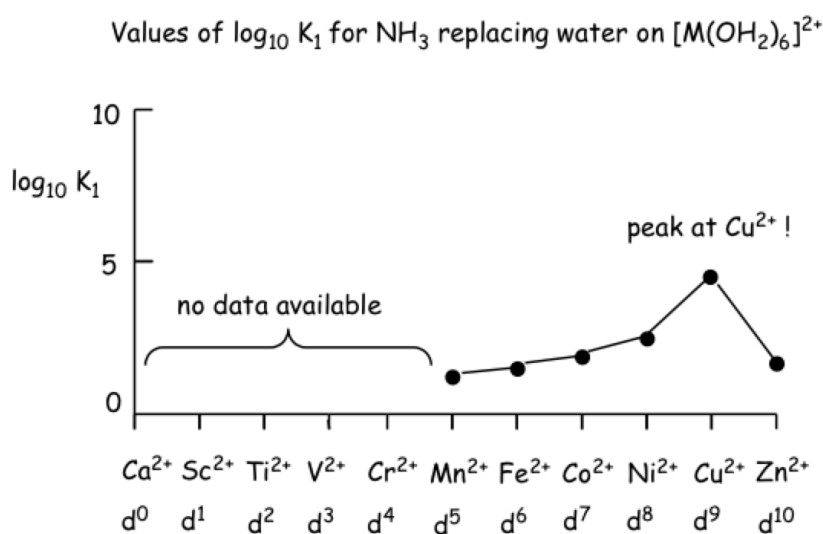
The Irving-Williams Series (IWS) describes an empirical increase in stability of M^{2+} octahedral complexes as a function of atomic radius, regardless of the nature of L for the following reaction:

$$[M(H_2O)_n]^{2+} \; + \; L \; \rightleftharpoons \; [M(H_2O)_{n-1}L]^{2+} \; + \; H_2O$$

$$K_1 \text{ varies along: } Ba^{2+} < Sr^{2+} < Ca^{2+} < Mg^{2+} < Mn^{2+} < Fe^{2+} < Co^{2+} < Ni^{2+} < Cu^{2+} < Zn^{2+}$$

As is evident from the above right figure, there is a maximum at Cu^{2+}, regardless of ligand. The series generally follows electrostatic effects whereby a smaller metal with same charge = greater charge density and this leads to tighter binding between the ligand and the metal. However, if we base binding strength purely on electrostatics then we would expect stabilities to vary in accordance with trends in ionic radius. So the trend in stabiltity would follow: $Mn^{2+} < Fe^{2+} < Co^{2+} < Ni^{2+} > Cu^{2+} > Zn^{2+}$. The reason Cu^{2+} is actually more stable than Ni^{2+} is due to the **Jahn Teller Distortion.**

6.1 *JAHN-TELLER DISTORTION.*

Jahn-Teller (J-T) distortion occurs when there is the possibility to asymmetrically fill orbitals that are degenerate in a non-linear complex. The geometry of the complex then distorts to reach a more stable electronic configuration. J-T distortion most commonly occurs for high spin d^4 $t_{2g}^3 e_g^1$ metals and low spin d^7 $t_{2g}^6 e_g^1$ metals or for d^9 $t_{2g}^6 e_g^3$ metals, all of which have an asymmetrically filled e_g set of orbitals. For Cu^{2+}, which is d_9, if there are 2 electrons in the d_{z2} and 1 electrons in the d_{x2-y2} orbital then there will be greater repulsion along the z-axis and therefore elongation of these M-L bonds along the z-axis to compensate, leading to stabilization of the d_{z2} orbital, which is the *most commonly observed distortion.* The M-L bonds along the xy plane by contrast contract, which leads to a destabilization of both the d_{xy} and d_{x2-y2} orbitals. This is illustrated in the figure below.

Compressed D_{4h} — Octahedral O_h — Elongated D_{4h}
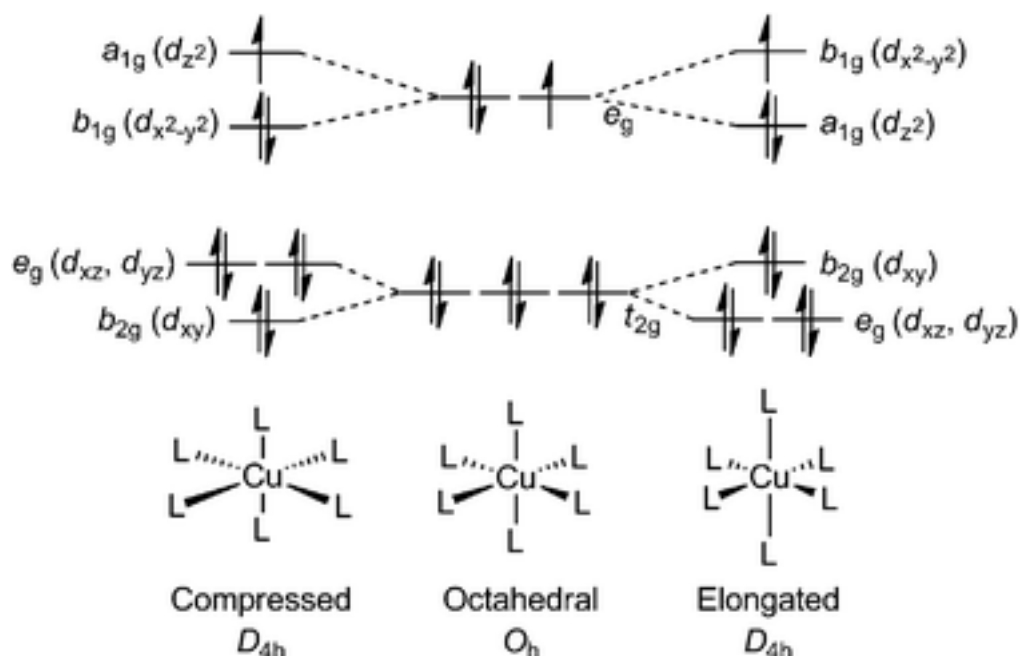
If there are 2 electrons in the d_{x2-y2} and 1 electron in d_{z2} then greater repulsion exists along the xy-plane and therefore there is effective compression of the M-L bonds along the z-axis to compensate and elongation of M-L bonds in the xy plane, leading to stabilization of the d_{x2-y2} orbital and the d_{xy} orbital; the d_{z2} orbital by contrast is destabilized.
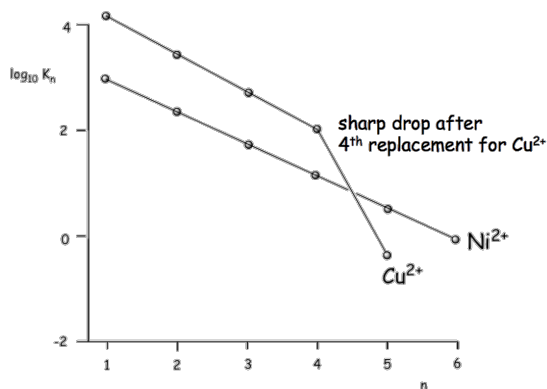
The presence of only **one electron** in the d_{x2-y2} orbital strengthens the water ligand attraction in the equatorial plane due to lower e^--e^- repulsion with the donor O electrons. The result is a raising in log K_{1-4} and a lowering in log K_5 and K_6 for ligand substitution of water molecules compared to the two ions either side; Ni^{2+} (d^8) and Zn^{2+} (d^{10}) where there is no such extra stabilization (see figure left).

7. THE CHELATE EFFECT.

Let's now consider the situation when the ligand L replacing coordinated water possesses two donor atoms that leads to the formation of a **chelate** ring. The figure below shows that the replacement of NH_3 on M^{2+}_{aq} by the chelates en (ethylene diamine) and EDTA (ethylene diamine tetraacetate) is thermodynamically favourable. This is a general phenomenon called the **chelate effect.**
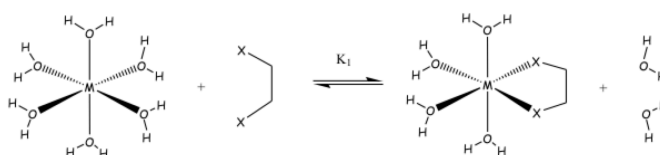
The increase in log K_1 as chelate rings are formed is a reflection of a more negative value of ΔG^o_1. It is largely due to an **increase in the entropy** of reaction i.e.
ΔS^o_1 is large and positive ($\Delta G^o_1 = \Delta H^o_1 - T\Delta S^o_1$).

Let's look at a specific example: $Ca^{2+}_{aq} + EDTA^{4-}$

Values of $\log_{10} K_1$ for various L replacing water on $[M(OH_2)_6]^{2+}$
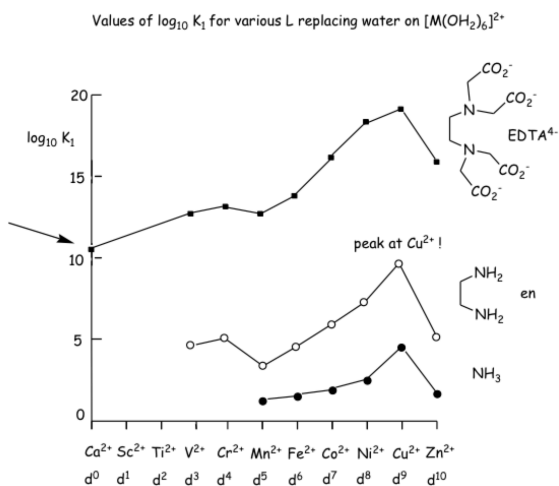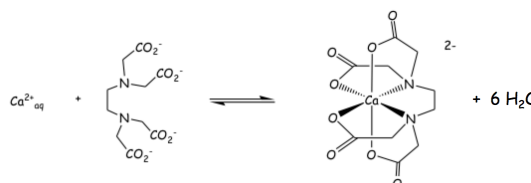
$\Delta G^o_1 = -60.5$ KJ mol^{-1}; $\Delta S^o_1 = 117$ J mol^{-1} K^{-1}
At 300 K, $\Delta H^o_1 = -25.4$ KJ mol^{-1} ($\Delta H^o_1 = \Delta G^o_1 + T\Delta S^o_1$)
Therefore, this complexation is mostly entropy driven ($T\Delta S^o_1 = -35.1$ KJ mol^{-1}), though there is a favourable enthalpic term as well (HSAB and chelate effect).

Why entropy controlled? There is an increase in entropy due to release of 6 water molecules, which leads to an increase in disorder of the system (i.e. 2 reacting molecules, 7 product molecules).

We can now calculate K_1 as $\Delta G^o_1 = -RT \ln (K_1)$ and
$\log(K_1) = \log (e^{-\Delta G1/RT}) = 10.53$.

$[Ni(NH_3)_6]^{2+} + 3$ en $\underset{}{\overset{\beta_3}{\rightleftharpoons}}$ $[Ni(en)_3]^{2+} + 6$ NH_3

4 species   7 species

Let's look at another specific example:
$[Ni(NH_3)_6]^{2+} + 3$ en

ΔG^o_1 = -57.2 KJ mol^{-1}; ΔH^o_1 = -16.6 KJ mol^{-1}; $-T\Delta S^o_1$ = -36.1 KJ mol^{-1}

Here both both enthalpy and entropy effects positively reinforce M-L binding. The **enthalpic effect** on chelation from **en** arises from stronger bonds to the **N** donors of the chelate as a result of the formation of the ring.

Let's look at another specific example where the enthalpy and entropy terms **do not** reinforce each other: Mg^{2+} + EDTA^{4-}

ΔG^o_1 = -51.2 KJ mol^{-1}; ΔH^o_1 = 13.8 KJ mol^{-1}; $-T\Delta S^o_1$ = -65.0 KJ mol^{-1}

Here the endothermic enthalpy term arises from the unfavourable replacement of two hard water ligands on the extremely hard Mg^{2+} by the softer N donors of EDTA^{4-} (HSAB). Formation of the chelate is however still highly favoured due to the favourable entropy contribution.

This begs the question why is Mg^{2+} harder than Ca^{2+}? Mg^{2+} is smaller (charge more concentrated) than Ca^{2+}, which will reinforce the electrostatic interaction (Hard-Hard) interaction with H_2O.

We can also probe the effect of the nature of the donor atom on the binding strength to the metal. The figure on the right illustrates that the **Order of log K_1 reflects HSAB theory.**

For Ni^{2+} to Zn^{2+} (soft metals): (soft) N^N > N^O > O^O (hard)
For Mn^{2+} (hard metal): (hard) O^O > N^O > N^N (soft)

Therefore, hard chelating ligands prefer to bind hard metals while soft chelating ligands prefer to bind soft metals. The "hardness" or "softness" of the ligand is based on the HSAB of the coordinating atoms. The table below provides compelling evidence of this HSAB effect in chelates.

T = 300K	$\Delta H°_1$ kJ mol^{-1}	$-T\Delta S°_1$ kJ mol^{-1}	$\Delta H°_1$ kJ mol^{-1}	$-T\Delta S°_1$ kJ mol^{-1}	$\Delta H°_1$ kJ mol^{-1}	$-T\Delta S°_1$ kJ mol^{-1}
Mn	-11.7	-3.8	-1.3	-16.9	+15.4	-34.2
Fe	-21.3	-6.4	-	-	-	-
Co	-28.9	-8.7	-11.7	-17.2	+12.1	-33.9
Ni	-37.2	-10.8	-20.5	-14.9	+7.9	-31.5
Cu	-54.4	-16.3	-25.9	-23.1	+11.9	-44.4
Zn	-28.0	-8.4	-13.8	-15.9	+13.1	-35.1
	$\Delta H°$ and $-T\Delta S°$ terms reinforce		$\Delta H°$ and $-T\Delta S°$ terms reinforce		complexation is entropy favoured only	

increasing hardness →

increasing softness ↓
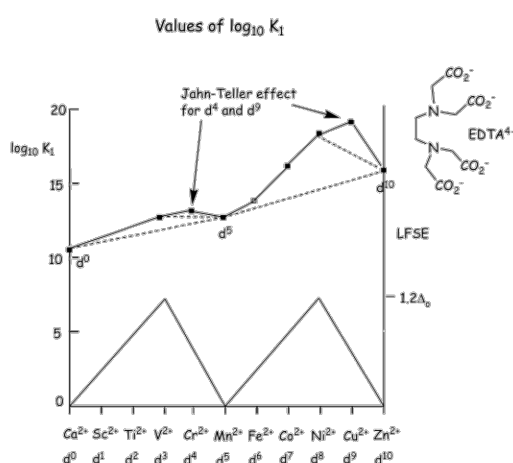
Binding strength is also influenced by the number of d electrons on the metal (LFSE), which is illustrated in the figure to the left. Here the trend in log K_1 mirrors the LFSE trends.

Ignoring LFSE, increasing K_1 reflects stronger M-L bonding as a function of increasing charge density on the M as the ionic radius decreases along the period.

Recall that the ionic radius decreases along the period is a result of the poor shielding of the nuclear charge by the addition of the successive d–electrons.

The d-orbitals do not penetrate into the nucleus because the d orbital wave function goes to zero before the nucleus is reached. This is called the d-block contraction.

7.1 *THE CHELATE EFFECT - APPLICATIONS.*

Chelation therapy has been used to treat diseases and conditions relating to metal overload. One example is Wilson's disease. Wilson's disease is a recessive genetic disorder that causes epilepsy amongst other neurological symptoms and is due to an overload of copper.

Chelating agents such as those to the right that bind Cu^{2+} ions strongly have been successfully used clinically to treat the condition.
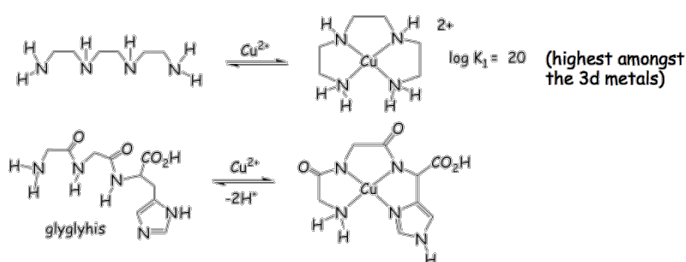
Another example involves chelation of Fe^{3+}. A potentially fatal condition called **hemosiderosis** occurs when the naturally occurring iron carrier protein **transferrin** becomes saturated and iron becomes deposited within the body.

In cases of severe iron overload, deposition in the heart, liver and endocrine systems leads to functional impairment of these organs, and reduced life expectancy.

Deferasirox
(tridentate)

manufactured as 'Exjade' by Novartis

excreted

There exist other clinically proven agents for the removal of Fe^{3+} from the body, such as deferoxamine and deferiprone and the examples shown below, which are all agents based on EDTA derivatives. Note in each example the affinity of the hard Fe^{3+} for hard **O** donors.

Deferoxamine (hexadentate)

binds through deprotonated hydroxamate groups

Deferiprone (bidentate)

EDTA⁴⁻   HBED²⁻   HBPD²⁻   HBHPD²⁻

US Patent 4528196

8. *STABILITIES OF OXIDATION STATES.*

The higher oxidation states become more oxidising and the lower oxidation states less reducing as one moves to the right of the d-block. Why is this so? It is due to the poor shielding of the nucleus by the addition of successive d-electrons (d block contraction), where the effective positive charge felt by an outer electron increases from left to right.

This has two consequences:
*   General decrease in ionic radius from left to the right.
*   Valence electrons become harder to lose/share the more to the right one goes.

Therefore, the higher oxidation states become more oxidizing and the lower states less reducing.

But how do we truly define the term **"oxidation state"**?
In nomenclature terms this is done by assuming octet configurations to define the charge on the atoms attached to the metal in the ion or complex. The table below provides some examples with different metals and ligand for what the calculated oxidation state on the metal would be.

Complex	Ligand	Total Charge on Ligand	Overall Charge on Complex	Oxidation State of Metal

$[Mn(OH_2)_6]^{2+}$	H_2O	0	+2	II
MnO_4^-	O^{2-}	8-	-1	VII
$[Fe(CN)_6]^{4-}$	CN^-	6-	-4	II
$[Co(NH_3)_4(O_2CR)Cl]^+$	NH_3 RCO_2^- Cl^-	0 1- 1-	+1	III

In reality, oxidation states are a formalism and are only true if the M-L bonding is highly ionic (electrostatic).

$$e.g., [Mn(OH_2)_6]^{2+} \text{ where Mn truly is Mn}^{2+}$$

where independent evidence exists from optical spectroscopy & magnetism that Mn^{2+} is high spin d^5.

$Mn^{7+}(O^{2-})_4$ $Mn^{6+}(O^{2-})_3(O^{-}\cdot)$ $Mn^{5+}(O^{2-})_2(O^{-}\cdot)_2$
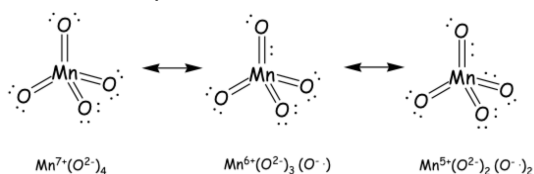
But what about the case of $[MnO_4]^-$ where the Mn-O bonds are highly covalent (Mn-O bond length is less than sum of ionic radii). So where now are the electrons (see the three resonance structures to the left)?

Here optical spectroscopy and magnetism are less informative:
- The absorption spectrum is dominated by O→Mn ligand-to-metal charge transfer bands
- The complex is diamagnetic

So we write as $Mn^{VII}(O^{-II})_4$

8.1 *QUANTIFICATION OF OXIDIZING AND REDUCING STRENGTHS.*

We know that MnO_4^- is a powerful oxidant and $[Cr(OH_2)_6]^{2+}$ is a powerful reductant. But how do we quantify oxidising and reducing strength? **The answer:** Using a scale of standard redox potentials, E_o.

These are best envisaged as part of an electrochemical cell – the driving force in a battery (shown to the right).
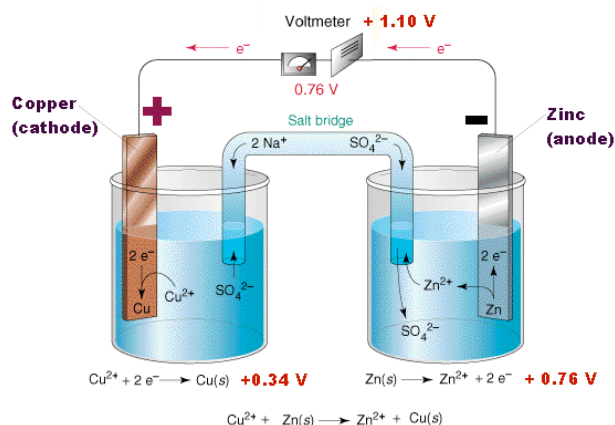
Consider the interaction of Cu^{2+}/Cu and Zn^{2+}/Zn in the **Daniell Cell.** The reaction is spontaneous as ΔG^o is negative.

This electrochemical cell can be thought of as two half reactions. The potential difference, E^o_{cell} is measured by the voltmeter.

The potential difference, E^o_{cell} is defined as the standard cell potential under standard conditions, which are:

$$Cu^{2+}_{aq} + 2\,e^- \rightleftharpoons Cu(s) \qquad E^o_{Cu(II)/Cu}$$

$$Zn^{2+}_{aq} + 2\,e^- \rightleftharpoons Zn(s) \qquad E^o_{Zn(II)/Zn}$$

- Unit activity (which means dilution solutions so activities approximate concentrations)
- 1 bar pressure of any gaseous component
- All solid components are in their standard states
- T = 298 K

The free energy of the cell, ΔG^{o}_{cell} = $-nFE^{o}_{cell}$
    where F is the Faraday constant = 96,487 C mol^{-1}
    n is the number of electrons transferred in the reaction

For a cell reaction to be thermodynamically favourable E^{o}_{cell} must be positive so that ΔG^{o}_{cell} is negative.

In the Daniell Cell, E^{o}_{cell} at 298 K = 1.10 V (see figure on previous page). This 1.10 V is comprised of: +0.34 V driving the reaction due to reduction of Cu^{2+} and +0.76 V driving the reaction due to oxidation of Zn(s). Where do these values come from?

Firstly, ΔG^{o}_{cell} = $-nFE^{o}_{cell}$ = -2*96,487*1.10 = -212 267 J per mol reaction = -212 kJ mol^{-1}, which demonstrates that the reaction for the oxidation of the zinc and the reduction of the copper is spontaneous.

All E^{o} values are related on a scale to the cell potential of the standard hydrogen electrode (SHE), which is arbitrarily set at a value of 0.0 V (think of this as analogous to ^{1}H NMR where every other resonance is reported relative to TMS). The SHE consists of platinum wire that is connected to a Pt surface in contact with an aqueous solution containing 1 M H^{+} in equilibrium with H_2 gas at a pressure of 1 atm. The half-cell potentials are **intensive properties**, namely *independent of the amount of the reacting species*. All half-reactions are written as reductions (only reactants are oxidizing agents and only products are the reducing agents). The more positive the E^{o} value the more readily the reaction occurs. The half-cell that has the more positive E^{o} value acts as the cathode.

By combining the SHE with another half-cell, e.g., $Cu^{2+}_{aq}/Cu(s)$ as in the Daniell cell, the E^{o} can be determined from the measured cell potential E^{o}_{cell}. Thus, in the Daniell cell:

$$Cu^{2+}_{aq} + 2e^{-} \rightleftharpoons Cu(s) \qquad E^{o}_{Cu(II)/Cu} = +0.34\ V$$

$$Zn^{2+}_{aq} + 2e^{-} \rightleftharpoons Zn(s) \qquad E^{o}_{Zn(II)/Zn} = -0.76\ V$$
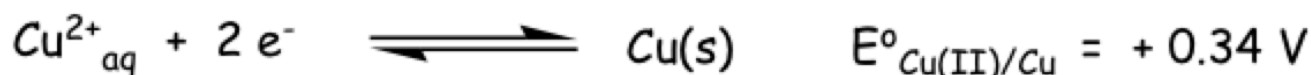
We can now see why Zn(s) readily reduces Cu^{2+}_{aq} and provides the huge driving force for the **Daniell cell**. Zn(s) thus is the stronger reducing agent and Cu^{2+} is the stronger oxidizing agent.

Let's look at a different reaction. Let's consider the well-known titration reaction of the reduction MnO_4^{-} with Fe^{2+}_{aq} under standard conditions (1 M H^{+}, 298 K).

The half reactions are:

$$Fe^{3+}{}_{aq} + e^- \rightleftharpoons Fe^{2+}{}_{aq} \qquad E^o = +0.77 \text{ V}$$

$$MnO_4{}^-{}_{aq} + 8 H^+{}_{aq} + 5 e^- \rightleftharpoons Mn^{2+}{}_{aq} + 4 H_2O \text{ (l)} \quad E^o = +1.51 \text{ V}$$

We can now see that from the relative E^0 values that the spontaneous reaction is:

$$MnO_4{}^-{}_{aq} + 8 H^+{}_{aq} + 5 Fe^{2+}{}_{aq} \overset{E^o{}_{cell}}{\rightleftharpoons} Mn^{2+}{}_{aq} + 5 Fe^{3+}{}_{aq} + 4 H_2O \text{ (l)}$$
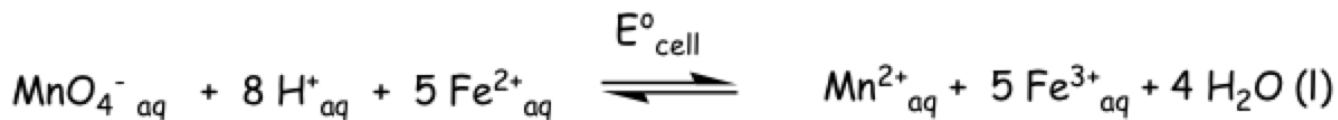
As $E^o{}_{cell} = E^o{}_{red} - E^o{}_{ox} = 1.51 - (+0.77) = 0.74$ V and $\Delta G^o{}_{cell} = -357.03$ kJ mol^{-1} (so is very favourable).

Let's now look at a different process, which is the oxidation of Fe(s) by $Cl_2{}_{aq}$.

The half reactions are:

$$Fe^{2+}{}_{aq} + 2 e^- \rightleftharpoons Fe(s) \qquad E^o = -0.44 \text{ V}$$

$$Fe^{3+}{}_{aq} + 3 e^- \rightleftharpoons Fe(s) \qquad E^o = -0.04 \text{ V}$$

$$Cl_2{}_{aq} + 2 e^- \rightleftharpoons 2 Cl^-{}_{aq} \qquad E^o = +1.36 \text{ V}$$
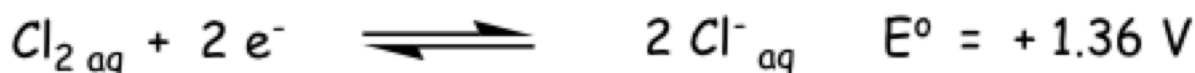
These data indicate that two reactions are possible:

$$Cl_2{}_{aq} + Fe(s) \rightleftharpoons 2 Cl^-{}_{aq} + Fe^{2+}{}_{aq} \qquad E^o{}_{cell} = +1.80 \text{ V}$$

$$3Cl_2{}_{aq} + 2 Fe(s) \rightleftharpoons 6 Cl^-{}_{aq} + 2 Fe^{3+}{}_{aq} \qquad E^o{}_{cell} = +1.40 \text{ V}$$
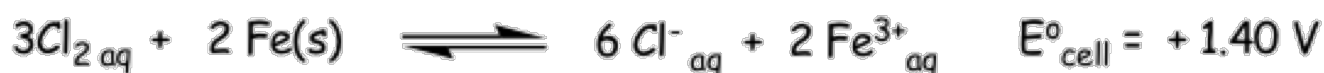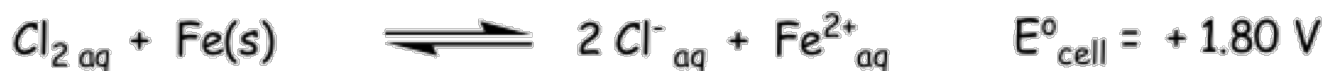
Both $E^o{}_{cell}$ values are positive and from their magnitude one might suppose the first reaction is favoured over the second but what really counts is the sign of $\Delta G^o{}_{cell}$.

It can be shown that the second reaction is favoured by consider the $\Delta G^o{}_{cell}$ values for the two processes, which take into account the number of electrons involved. The first reaction involves two electrons while the second reaction involves six electrons. Recall that $\Delta G^o{}_{cell} = -nFE^o{}_{cell}$.

$$Cl_{2\ aq} + Fe(s) \rightleftharpoons 2\ Cl^-_{\ aq} + Fe^{2+}_{\ aq} \qquad E^o_{cell} = +1.80\ V$$
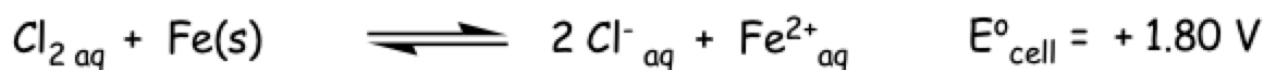
$$\Delta G^o_{cell} = -n\ F\ E^o_{cell} = -2 \times 96487 \times 1.80 = -347\ kJ\ mol^{-1}$$

$$3Cl_{2\ aq} + 2\ Fe(s) \rightleftharpoons 6\ Cl^-_{\ aq} + 2\ Fe^{3+}_{\ aq} \qquad E^o_{cell} = +1.40\ V$$
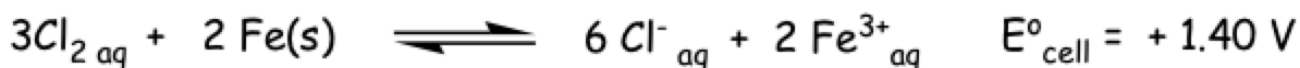
$$\Delta G^o_{cell} = -n\ F\ E^o_{cell} = -6 \times 96487 \times 1.40 = -810\ kJ\ mol^{-1}$$

Therefore second reaction favoured by **~ 500 kJ mol^{-1} !**

8.1.1 *QUANTIFICATION OF OXIDIZING AND REDUCING STRENGTHS UNDER NON-STP CONDITIONS.*

So far we have been looking at systems under standard conditions. What happens if we change the pH?

Let look at this first example: Reduction of MnO_4^-.

$$MnO_4^-{}_{aq} + 8\ H^+_{\ aq} + 5\ e^- \rightleftharpoons Mn^{2+}_{\ aq} + 4\ H_2O\ (l) \qquad E^o = +1.51\ V$$

Here E^o refers to the condition $[H^+] = 1\ mol\ dm^{-3}$, pH = 0. Because of the consumption of H^+ ions, the above E^o will vary with pH. What would be the measured E value for the above at pH 2.5 at 298 K?

We can calculate E under any conditions using the **Nernst Equation**.

$$oxidant + n\ e^- + y\ H^+ \rightleftharpoons reductant$$

$$E_{measured} = E^o_{standard} - \frac{R\ T}{n\ F} \ln\left(\frac{[reductant]}{[oxidant]\ [H^+]^y}\right)$$

For the reduction of MnO_4^-:

$$E_{measured} = 1.51 - \frac{R\ T}{n\ F} \ln\left(\frac{[Mn^{2+}_{\ aq}]}{[MnO_4^-]\ [H^+]^8}\right)$$

At pH = 2.5 = $-\log_{10}([H^+])$; $[H^+] = 3.2 \times 10^{-3}$ M:

$$E_{measured} = 1.51 - \frac{8.314 \times 298}{5 \times 96487} \ln\left(\frac{[Mn^{2+}_{aq}]}{[MnO_4^-][3.2 \times 10^{-3}]^8}\right)$$

At the mid point $[Mn^{2+}_{aq}] = [MnO_4^-]$ and $E = E_{eq}$

$$E_{eq} = 1.51 - 5.13 \times 10^{-3} \ln(2.98 \times 10^{12})$$

= 1.27. This implies that E_{cell} drops as the pH increases.

Let's look at a second example: Reduction of Zn^{2+}_{aq}

		$E^o_{Zn(II)/Zn}$	
		pH 0	pH 14
$Zn^{2+}_{aq} + 2e^- \rightleftharpoons Zn(s)$		-0.76 V	-1.20 V
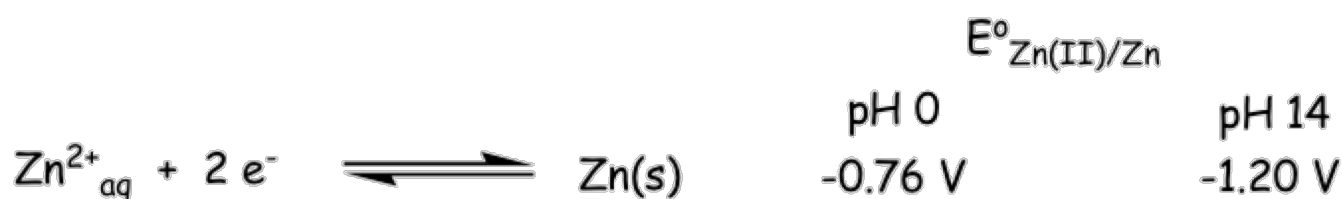
In this reaction there is no $[H^+]$ consumption. So why is there a change in the cell potential? The reason is that at pH 0 the Zn^{2+} species is $[Zn(OH_2)_6]^{2+}$ but at pH 14 the species is $[Zn(OH)_4]^{2-}$. So the Zn^{2+} species being reduced is different!

Let's now look at a third example: Mn^{3+}/Mn^{2+}_{aq} – an example where pH affects redox behavior.
At **pH 0**: Mn^{3+} exists as $[Mn(OH_2)_6]^{3+}$ and can oxidise $H_2O \rightarrow O_2$.

$$[Mn(OH_2)_6]^{3+} + e^- \rightleftharpoons [Mn(OH_2)_6]^{2+} \quad E^o = +1.54 \text{ V}$$

$$O_2 + 4H^+ + 4e^- \rightleftharpoons 2H_2O \quad E^o = +1.23 \text{ V}$$

E^o_{cell} = 1.54 - 1.23 = 0.31 V (favourable) and $\Delta G^o_{cell} = -nFE^o_{cell} = -4*96487*0.31$ J mol^{-1} = -120 kJ mol^{-1}

At **pH 14**: Mn^{III} and Mn^{II} are now present as the hydroxo complexes; $Mn(OH)_{2/3}(s)$ and so the speciation is different under basic conditions compared to acidic conditions. Recall that at pH = 14 $[OH^-]$ = 1 mol dm^{-3}.

$$Mn(OH)_3(s) + e^- \rightleftharpoons Mn(OH)_2(s) + OH^-_{aq} \quad E^o = -0.27 \text{ V}$$

$$O_2 + 2H_2O + 4e^- \rightleftharpoons 4OH^-_{aq} \quad E^o = +0.40 \text{ V}$$

Now O_2 is the oxidant and E^o_{cell} = 0.4 – (-0.27) = 0.67 V (favourable) and $\Delta G^o_{cell} = -nFE^o_{cell} = -4*96487*0.67$ J mol^{-1} = -259 kJ mol^{-1}

8.1.2 LATIMER DIAGRAMS.

When several oxidation states exist for a particular metal a convenient method of representing the respective E^o values is in the form of a Latimer diagram.

With multiple Latimer diagrams, one can illustrate the change in E^o with pH.

The first example is for Fe at pH = 0 (left) and pH = 14 (right).

+3	+2	0	+6	+3	+2	0
$Fe^{3+}(aq)$	$Fe^{2+}(aq)$	$Fe(s)$	$FeO_4^{2-}(aq)$	$Fe(OH)_3(s)$	$Fe(OH)_2(s)$	$Fe(s)$
+0.77	-0.44		+0.81	-0.86	-0.89	
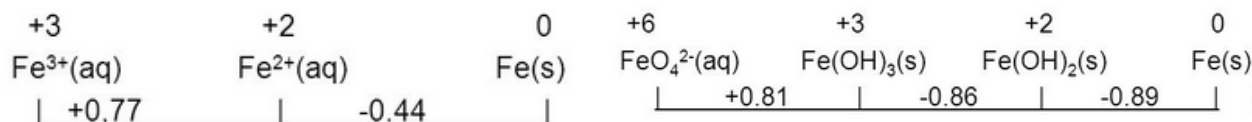
Using ΔG^o values for each step we can show using the above left Latimer diagram that $E^o(Fe^{3+}_{aq}/Fe(s))$ = -0.04 V. See if you can calculate what $E^o(FeO_4^{2-}/Fe(s))$ should be. Recall Hess' law:

$$\Delta G_{overall} = \Sigma\ \Delta G_{individual\ steps}$$

The second example is for Mn where the top Latimer diagram is at pH = 0 and the bottom Latimer diagram is at pH = 14.
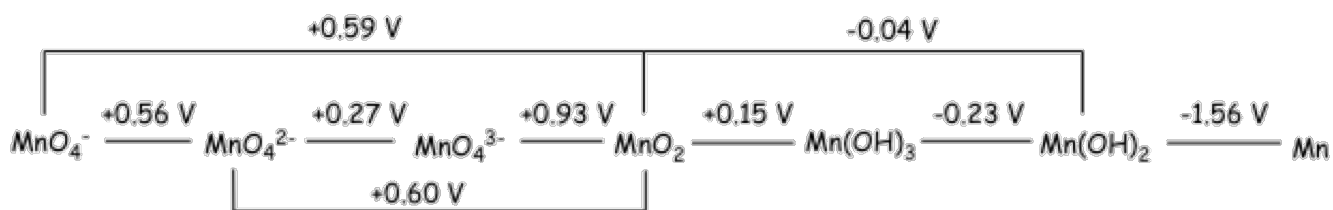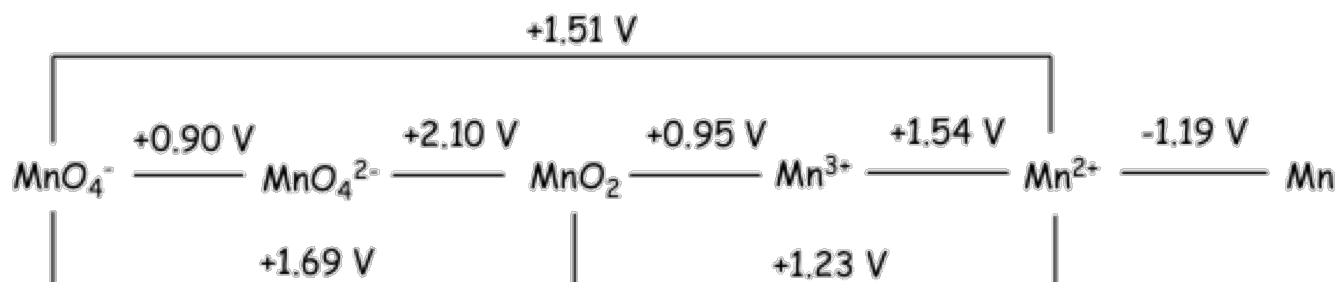
When a given oxidation state has a higher (more positive) E^o for its **reduction** (i.e. the number to the right of the complex) than for its oxidation (i.e. the number to the left of the complex) it is thermodynamically **<u>unstable</u>** to disproportionation to give the two species on either side of the complex in the Latimer diagram. One can show that ΔG^o for this process is negative. At pH = 0, MnO_4^{2-} and Mn^{3+} are both unstable to disproportionation while at pH = 14 MnO_4^{3-} will disproportionate to MnO_4^{2-} and MnO_2.

8.1.2 FROST-EBSWORTH DIAGRAMS.

Latimer diagrams are great and very descriptive. Another convenient way of representing redox behaviour is to graphically plot ΔG^o versus the oxidation number.

Recall that ΔG^{o} = - nFE^{o} and so $\Delta G^{o}/F$ = -nE^{o}

So if we plot nE^{o} vs oxidation number then the slope of the line drawn between two oxidation states, separation n, will give E^{o} for that process. The Frost Ebsworth diagram is a very good graphical tool that can be used to predict redox behaviour.
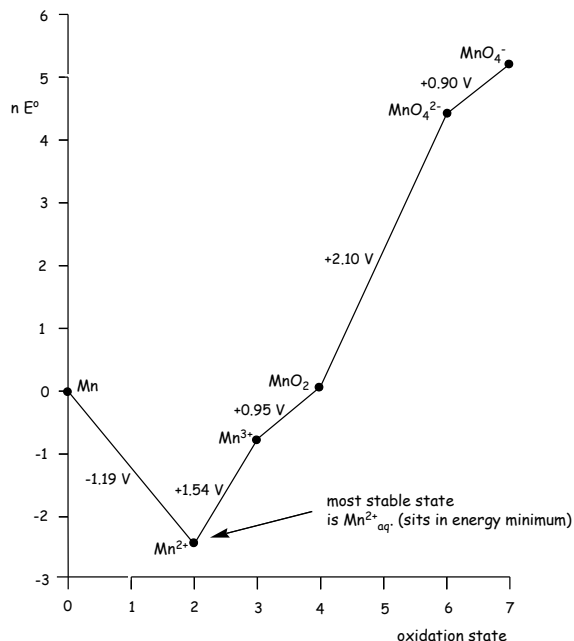
Let's now look at Mn at pH = 0. As nE^{o} becomes more negative the stability of the species increases. The further positive the nE^{o} is the more oxidizing the complex is. So MnO_4^- is the most oxidizing and Mn^{2+} is the most stable. Compounds that show a decrease convex behaviour (i.e. a decrease in the slope to the right of the complex compared to the left) are prone to disproportionation. Notice that this is the case for Mn^{3+} and MnO_4^{2-}.

Let's look more closely at the case for MnO_4^{2-} (remember we write the redox reactions as reductions).

$$MnO_4^{2-} + 4\,H^+ + 2\,e^- \rightleftharpoons MnO_2 + 2H_2O \quad E^o = +2.10V$$

$$MnO_4^- + e^- \rightleftharpoons MnO_4^{2-} \quad E^o = +0.90V$$

$$3\,MnO_4^{2-} + 4\,H^+ \rightleftharpoons MnO_2 + 2\,MnO_4^- + 2H_2O$$

The third equation shows the overall balanced equation, which is equation 1 + 2* equation 2 (equation 2 is inverted and so E^o becomes -0.9 V).
So E^o_{disp} = 2.10 – 0.90 = 1.20 V and ΔG^o = -nFE^o = -2*96487*1.2 = -231.5 KJ mol^{-1}.

Let's now look at how the redox behaviour changes at pH = 14. We can now observe that MnO_4 is much less oxidizing under basic conditions while $Mn(OH)_3$ becomes the most stable species.
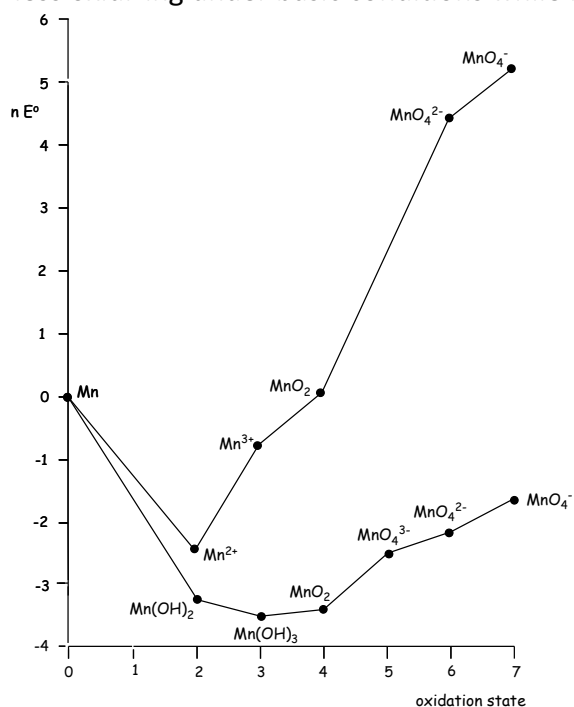
Which pH condition is best for MnO_4^- titrations?
At pH = 0 the use of acid solution avoids MnO_2(s) production.

So at pH = 14

	E^o / V	G^o / kJ mol^{-1}

$$MnO_4^-{}_{aq} + 8 H^+{}_{aq} + 5 e^- \rightleftharpoons Mn^{2+}{}_{aq} + 4 H_2O (l) \qquad +1.51 \qquad -728.5$$

$$MnO_4^-{}_{aq} + 4 H^+{}_{aq} + 3 e^- \rightleftharpoons MnO_2(s) + 2 H_2O (l) \qquad +1.69 \qquad -489.2$$
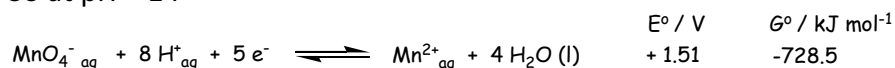
From there two equations we can see that the reduction to Mn^{2+}(aq) is favoured.

Note that in air (so with O_2)

$$O_2 + 2 Mn^{2+}{}_{aq} + 2 H_2O \rightleftharpoons 2 MnO_2(s) + 4 H^+{}_{aq} \qquad 0.0 \qquad 0$$

At pH = 14

$$MnO_4^-{}_{aq} + 4 H_2O + 5 e^- \rightleftharpoons Mn(OH)_2(s) + 6 OH^-{}_{aq} \qquad +0.34 \qquad -164$$

$$MnO_4^-{}_{aq} + 2 H_2O + 3 e^- \rightleftharpoons MnO_2(s) + 4 OH^-{}_{aq} \qquad +0.59 \qquad -170.8$$
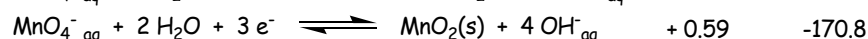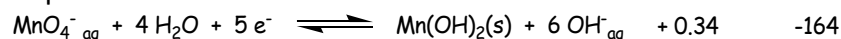
From there two equations we can see that the reduction to MnO_2 is favoured.
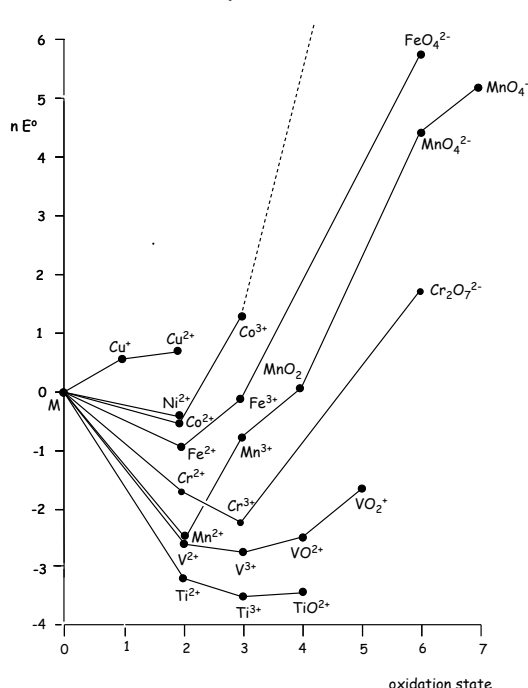
Note that in air (so with O_2)

$$O_2 + 2 Mn(OH)_2(s) \rightleftharpoons 2 MnO_2(s) + 2 H_2O \qquad +0.44 \qquad -169.8$$

Let's now look at a Frost Ebsworth diagram along the 3d series of the periodic table. Note how the lower oxidation states become more stable and less reducing along the period.

Note that copper is the first truly inert 3d metal (all E^o values are positive. This is typical of coinage metals. Cu is the only 3d metal found naturally in its elemental form. We can also observe that Cu^+(aq) will disproportionate.

8.1.3 THE LINK BETWEEN OXIDATION POTENTIAL AND IONIZATION POTENTIAL.

The reduction of a metal in solution actually consists of three processes. $M^{2+}{}_{aq} + 2 e^- \rightleftharpoons M(s)$

Firstly, the metal solid needs to be atomized (or vapourized), for which there is an associated energy required to do so. Then, if we are discussing a two electron process, the atomized metal needs to be ionized twice (i.e. two electrons are removed). This corresponds to the first and second ionization potentials. Finally, this oxidized species needs to be solvated. As we are discussing chemistry in water, this solvation is called a hydration. There is an energy requirement with this process as well.

$$M(s) \longrightarrow M(g) \qquad \text{atomization} \qquad H^o{}_a$$

$$M(g) \longrightarrow M^{2+}(g) \qquad \text{ionization} \qquad (IP_1 + IP_2)$$

$$M^{2+}(g) \longrightarrow M^{2+}_{aq} \quad \text{hydration} \quad H^o_{hyd}$$
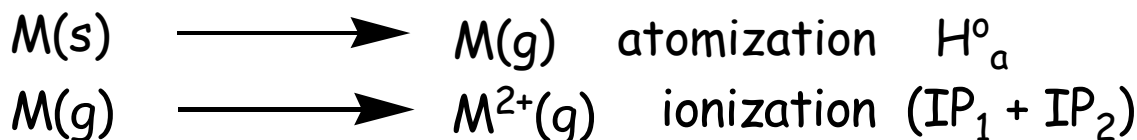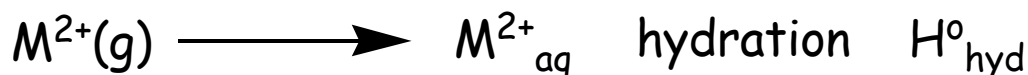
So do any of these processes correlate with trends in E^o? The answer is that the values of E^o correlate with the ionization potentials (IP1+IP2), as shown below. The expected variation of ΔH^o_{hyd} with LFSE (forming the aquo complexes) does not contribute significantly. The low E^o for Zn^{2+}/Zn does correlate however with an unusually low value of ΔH^o_a for $Zn(s)$.
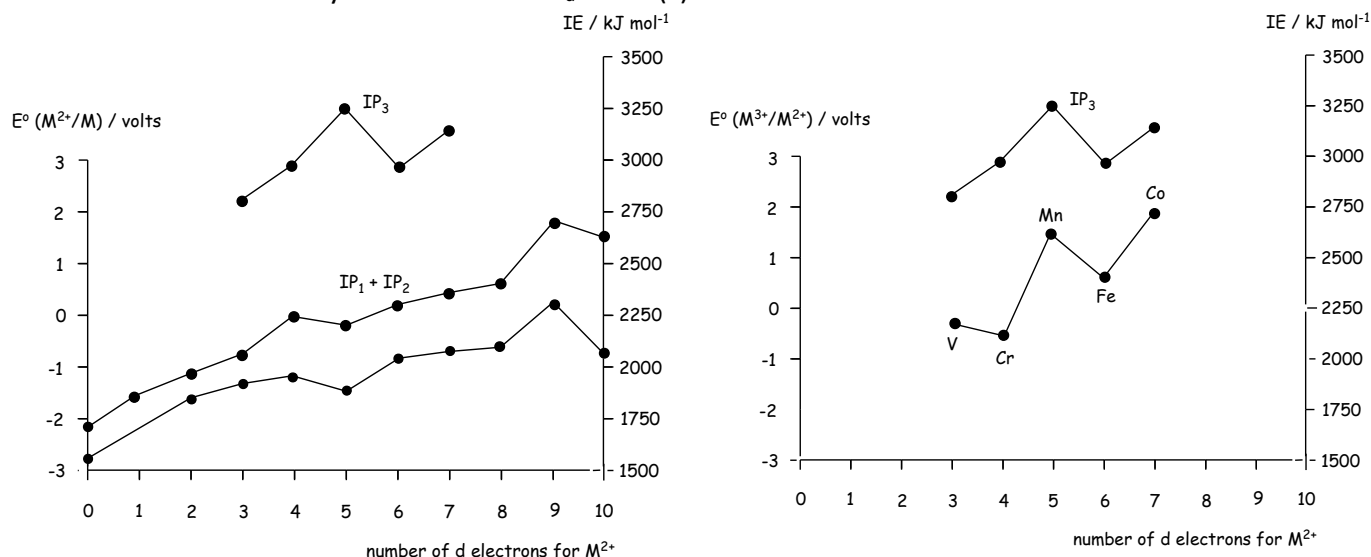
Furthermore, $E^o(M^{3+}/M^{2+})$ correlates with IP_3, with the exception of chromium (see figure above, right). Once again the variation in respective ΔH^o_{hyd} values of M^{2+} and M^{3+} is not significant.

On the basis of IP_3, oxidation of $Cr^{2+}(g)$ should be more difficult than of V^{2+} (g) by ca. 165 kJ mol^{-1} Yet Cr^{2+}_{aq} is a more powerful reductant (more negative E^o) than V^{2+}_{aq}. The reason is the considerable gain in LFSE (0.6 Δ_o) on forming the d^3 Cr^{3+} ion ($t_{2g}^3 e_g^0$ configuration).

Oxidation of V^{2+}_{aq} to V^{3+}_{aq} ($t_{2g}^3 e_g^1$ configuration) actually results in a loss of LFSE of 0.4 Δ_o compared to V^{2+}_{aq}.

M	M^{3+} LFSE units of Δ_o	M^{2+} LFSE units of Δ_o	Change in LFSE $M^{2+} \rightarrow M^{3+}$ units of Δ_o
V	-0.8	-1.2	0.4 loss
Cr	-1.2	-0.6	-0.6 gain

So in this case LFSE factors are significant. Mostly, LFSE factors do not play a significant role in determining trends in E^o.

9 RATES OF REACTIONS INVOLVING 3D TRANSITION METAL IONS IN AQUEOUS MEDIA.

Up until we have concentrated on thermodynamic stability. Let's now turn our focus to understanding the kinetics of these reactions and assess whether the kinetics of the reaction correlate with the thermodynamics of the reaction.

Consider the following processes:

cyclam
(macrocycle)

$\log\beta_1 = 19.4$

$\log\beta_4 = 22$

$$[Ni(OH_2)_6]^{2+} + 4\,CN^- \underset{}{\overset{\log 4}{\rightleftharpoons}} [Ni(CN)_4]^{2-} + 6\,H_2O \qquad \log\beta_4 = 22$$
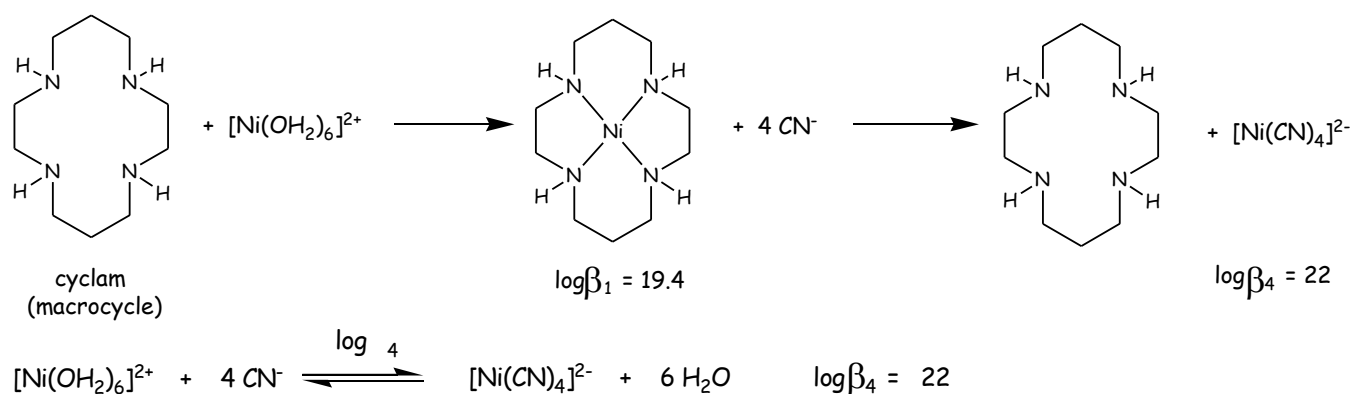
In both reactions, regardless of whether the ligand is a chelate cyclam or just water, these reactions have one of the largest log β_n values known for a monodentate ligand replacing H_2O. What this means is that $[Ni(CN)_4]^{2-}$ is very stable thermodynamically.

Now consider the rate of the reaction for the following process:

$$[Ni(CN)_4]^{2-} + {}^*CN^- \xrightarrow{k} [Ni({}^*CN)(CN)_3]^{2-} + CN^-$$

exchange of CN⁻ ligand
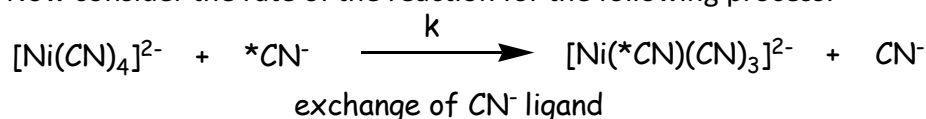
$$k = 2.3 \times 10^6 \ M^{-1}\ s^{-1}$$

- representing an exchange event every microsecond!!!

The rate constant, k, is very large and what this means is that $[Ni(CN)_4]^{2-}$ is very **labile**!

These experiments show that **thermodynamic stability** does not necessarily correlate with **kinetic inertness**. The attainment of equilibrium in metal ion complexation processes can be an extremely fast process; irrespective of the size of the stability constants: K_n or β_n. In fact, ms and μs timescale ligand exchange events involving monodentate ligands are common within 3d transition metal complexes.

A wide range of rates is relevant for ligand exchange reactions at metal complexes. Let's consider water exchange on the aqua species. For main group metal ions (shown below) these range from the most labile (Cs^+_{aq}, half-life = 1 ns) to the most inert (Al^{3+}_{aq}, half-life = 1 s), which corresponds to 9 orders of magnitude change in half life.

This is mostly as a result of variations in the metal ionic radius which affects the strength of the predominantly ionic (electrostatic) bonding to the coordinated waters.

	Ionic radius / pm	Water exchange half life / s
$[Be(OH_2)_4]^{2+}$	27	10^{-2}
$[Mg(OH_2)_6]^{2+}$	72	10^{-5}
$[Ca(OH_2)_7]^{2+}$	105	10^{-7}
$[Ba(OH_2)_8]^{2+}$	142	10^{-9}

	Ionic radius / pm	Water exchange half life / s
$[Al(OH_2)_6]^{3+}$	54	1
$[Ga(OH_2)_6]^{3+}$	62	10^{-3}
$[In(OH_2)_6]^{3+}$	80	10^{-6}

However, for the 3d transition metal ions **size is not the only factor**. Here there is no correlation with size. V^{2+} has the largest radius but it is the <u>most inert</u>. The half-lives (related to the **rates**) of exchange, just like the stability constants we saw earlier, **correlate** with **LFSE** not size.

	Ionic radius / pm	Water exchange half life / s
$[V(OH_2)_6]^{2+}$	79	10^{-2}
$[Co(OH_2)_6]^{2+}$	75	10^{-6}
$[Ni(OH_2)_6]^{2+}$	69	10^{-4}

Let's now look at the exchange rates for M^{2+} ions along the 3d series. The anomalously high rates for Cr^{2+}_{aq} and Cu^{2+}_{aq} reflect the rapid dynamics attached to the weakly-bonded water ligands within the Jahn-Teller distorted structures (see below). The exchange in these systems is so fast that exchange occurs every nanosecond.
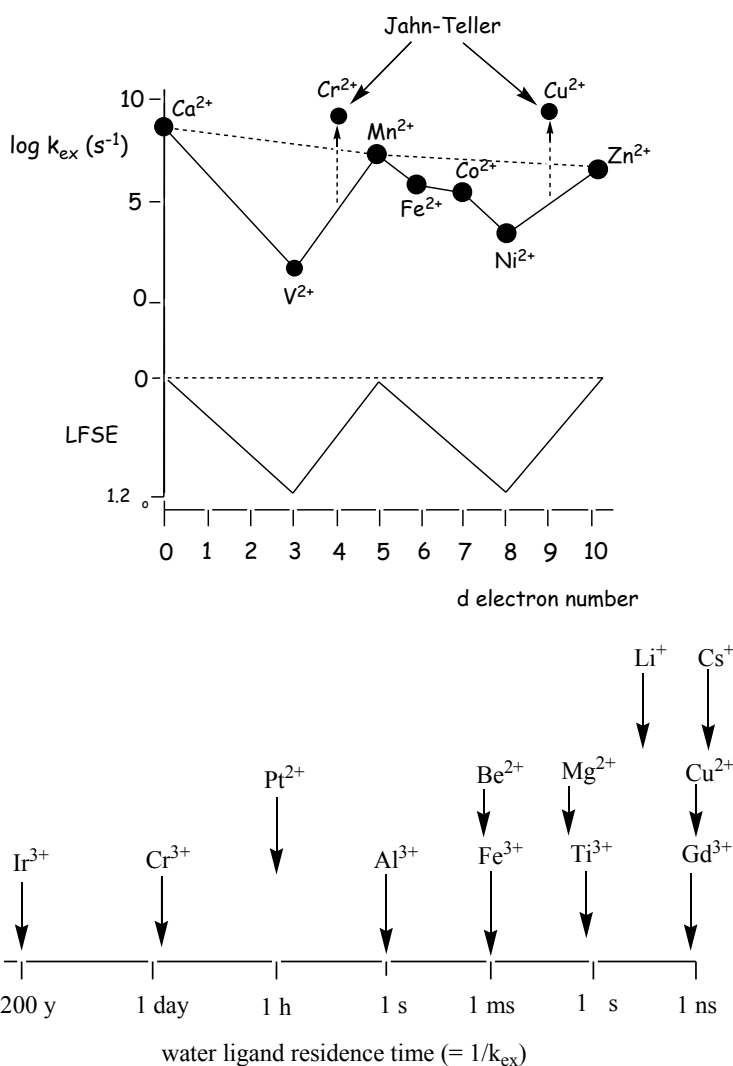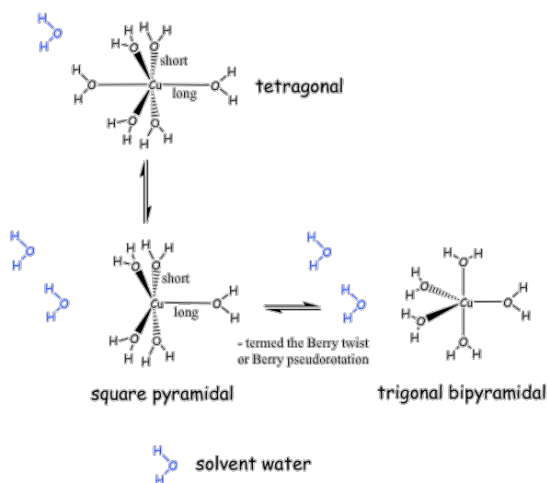
Amazingly, the rates of water ligand exchange on aqua metal ions across the periodic table cover <u>20</u> orders of magnitude (see right).

Generally:

Lower charge leads to faster exchange while higher charge leads to slower exchange. Similarly, larger ion size leads to faster exchange while smaller ion size leads to slower exchange. Ir^{3+} is rather large

and so doesn't fit within the aforementioned trend! Why is ligand exchange then so slow for this ion? Because it is in the 3rd row (5d metal complex) and so Δ_o is very large and so the CFSE is likewise very large leading to a very high ligand field activation energy (LFEA).

Ligands with exchange half-lives of less than a minute are normally labelled as **labile** while those with exchange half-lives of greater than a minute are labelled as **inert**.

So how was the exchange on Ir^{3+}_{aq} measured? Since water exchange involves bond breaking from M^{n+} to resident water, which has an endothermic activation barrier of about 130 kJ mol^{-1}, raising the temperature will speed up the reaction. In fact, water exchange on $[Ir(H_2O)_6]^{3+}$ was studied in pressurized vessels at <u>120 ^{o}C</u> where an event occurs now in less than 1 hour. The reaction can be followed by NMR using enriched ^{17}O-labelled water (^{17}O has an NMR signal like ^{1}H).

Of all the 3d transition metal aqua ions only **Cr^{3+}$_{aq}$** is classed as inert. Why is that? Octahedral $[Cr(H_2O)_6]^{3+}$
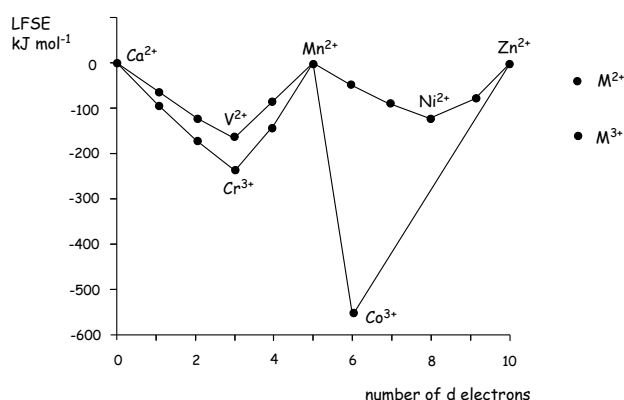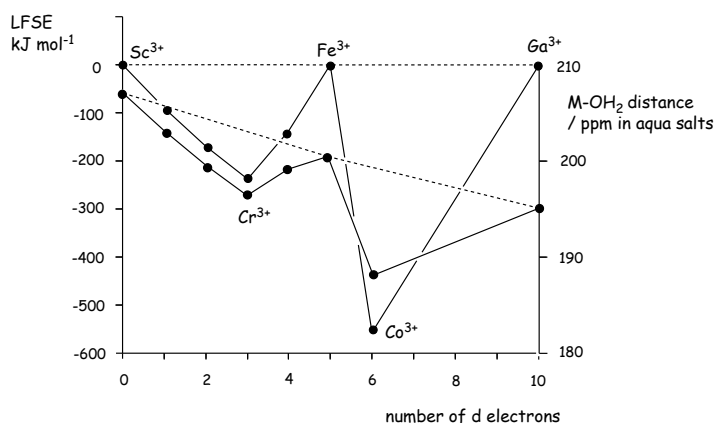
has a high charge coupled with a very stable t_{2g}^{3} configuration with $-1.2\Delta_o$ of LFSE. High LFSE correlates with a high ligand field activation energy (LFAE) for exchange, which translates to slow exchange. We can see this graphically to the right. From the graph, Co^{3+}aq should be the most inert. Why is this not the case. The value shown in the graph above presumes that $[Co(H_2O)_6]^{3+}$ has a low spin configuration where it has a high charge (high Δ_o) coupled with a t_{2g}^{6} configuration and therefore has the maximum LFSE possible of $-2.4\Delta_o$ and therefore also a high LFAE. The complex could have a high spin configuration and so Co^{3+} would then have a LFSE of only $-0.4\ \Delta_o$. Of course we could look at the magnetic properties to determine the electronic configuration of the cobalt ion but we can also tell from the M-OH$_2$ distances in the aqua complexes (see the graph to the left). The decrease in M-OH$_2$ distance once again reflects decreasing M^{3+} ionic radius across series.

The rate of exchange on $[Co(OH_2)_6]^{3+}$ has not been measured however because it is **not stable** as $[Co(OH_2)_6]^{3+}$ spontaneously oxidizes water to O_2. We can assess this from the E^{o} values and ΔG^{o}_{cell} = -nFE^{o}_{cell} = -4*96487*0.75 = -386 kJ mol^{-1}.

$$[Co(OH_2)_6]^{3+} + e^- \rightleftharpoons [Co(OH_2)_6]^{2+} \quad E^o = +1.98\ V$$

$$O_2 + 4H^+ + 4e^- \rightleftharpoons 2H_2O \quad E^o = +1.23\ V$$

The exchange reaction observed is catalysed by the more labile $[Co(OH_2)_6]^{2+}$ generated from the redox reaction shown above. $[Co(OH_2)_6]^{3+}$ provides another good example of the lack of correlation between

thermodynamic stability and kinetic lability. **[Co(OH₂)₆]³⁺ is inert yet only metastable**. Literally hundreds of stable Co^{3+} complexes are known with ligands other than water. Most of the ligands N-donor ligands. Because of their redox stability, coupled with slow rates of ligand exchange, many of these have played
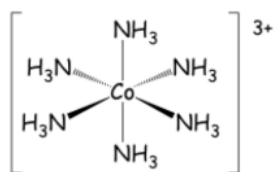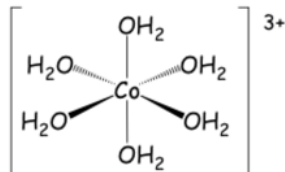
a huge role in developing our understanding of the mechanisms of reactions at transition metal centres. Why is there such a huge difference in E^o values between the two complexes on the left with Co^{III} stabilized hugely with N-donors like NH_3?

$$E^o\,(Co^{III/II}) = +0.1\ V$$

$$E^o\,(Co^{III/II}) = +1.98\ V$$

The reason relates back to the different ligands used. NH_3 (and other N-donor ligands) are σ-donors while water is a σ-donor π-donor ligand. The added π-donation raises the energy of the t_{2g} orbitals and reduces Δ_o. Moreover, water is a weaker σ-donor than NH_3 given the more electronegative coordinating oxygen atom. These effects decrease the stability of the *low spin* d⁶ configuration of $[Co(OH_2)_6]^{3+}$ (below left) with respect to it reduction to the *high spin* d⁷ $[Co(OH_2)_6]^{2+}$ ($\Delta_o < P$) (below right), thereby providing a vacancy in the t_{2g} set for an additional electron.
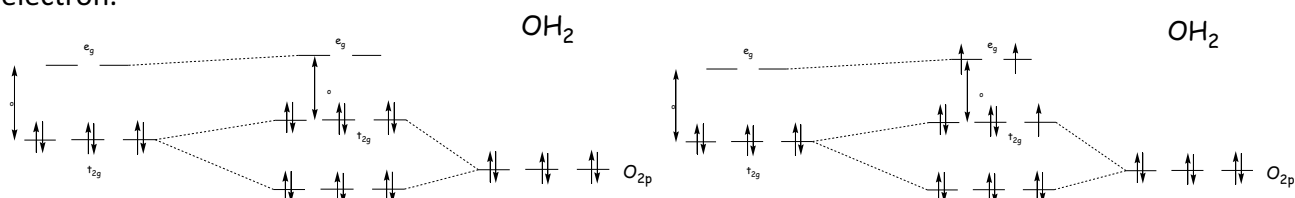
There are only two known high spin Co^{3+} complexes:

- $[Co(OH_2)_3F_3]$
- $[CoF_6]^{3-}$

This is due to good π-donation from F^-, which dramatically decreases Δ_o. All other Co^{3+} complexes are low spin, which is due to stronger σ-donation of the ligands outweighing all other effects.

10 *LIGAND EXCHANGE MECHANISMS.*

You all are familiar with substitution reactions on carbon: S_N1 and S_N2.

There exist comparable mechanisms for ligand replacement on the metal
- Dissociative – similar to S_N1
- Associative – similar to S_N2
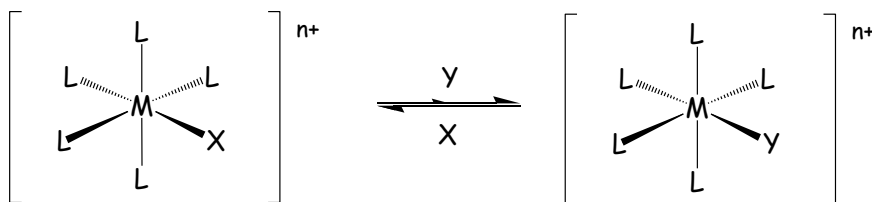
The Dissociative path: X leaves first, generating a coordinatively unsaturated complex, and then Y coordinates at the vacant site on the metal (shown below).
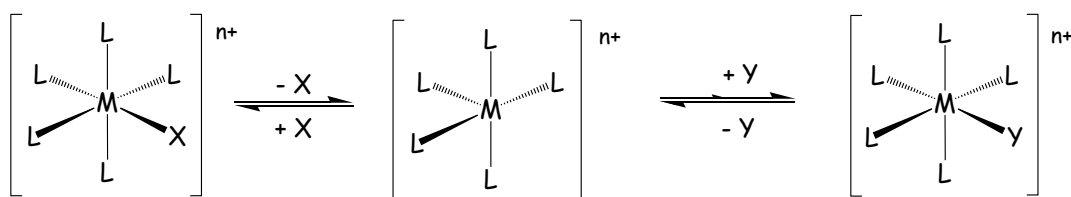
The Associative path: M-Y bond forms first, generating a congested complex, followed by de-coordination of X.
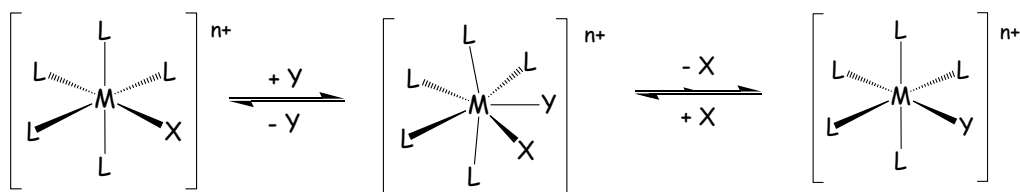
Which path would you predict to have the **largest** activation energy?

Answer: The dissociative path. Why?

This mechanism involves a bond-breaking step (M-X bond) in the rate determining step (RDS), which will be endothermic before the new bond is formed – formally this is a two-step reaction.

Analogously, S_N1 reactions are frequently slower than S_N2 reactions for the same reason.

The associative path involves a bond-making step (M-Y), which will be exothermic prior to bond breaking (M-X) and so should possess a lower activation energy.

Additionally, the presence of the new M-Y bond may lower to energy required to break the M-X bond

The activation energy E_a can be determined from the temperature dependence of the reaction rate according to the Arrhenius or Eyring equations.
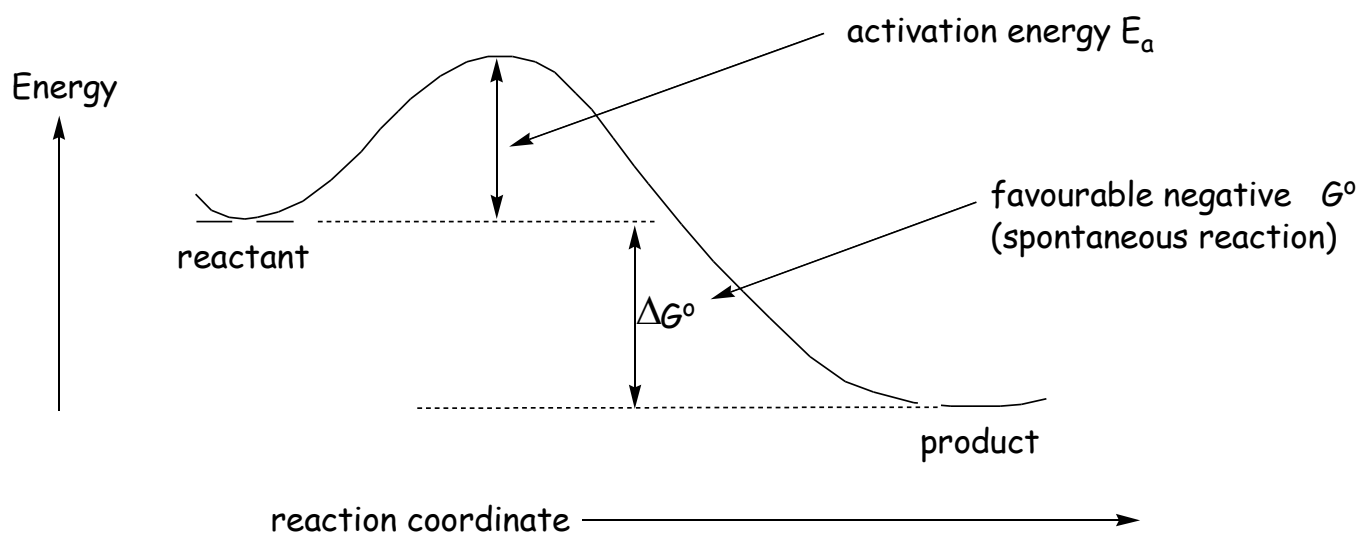
The Arrhenius equation is shown below, with the linearized form to the left. Notice that the slope is E_a/R, where R is the gas constant:

$$\ln k = \ln A - \frac{E_a}{RT} \qquad \text{or} \qquad k = A e^{\left(\frac{-E_a}{RT}\right)}$$

The related Eyring equation is shown below, where *k' and h* are the Boltzmann and Planck's constants, respectively:

$$\ln k = \ln\left(\frac{k'\,T}{h}\right) - \frac{\Delta G^{\ddagger}}{RT} \qquad \text{or} \qquad k = \left(\frac{k'\,T}{h}\right)e^{\left(\frac{\Delta G^{\ddagger}}{RT}\right)}$$

We can rearrange the Eyring equation to give:

$$\ln k = \ln\left(\frac{k'\,T}{h}\right) - \frac{\Delta G^{\ddagger}}{RT} \longrightarrow \ln k = \ln T + \ln\left(\frac{k'}{h}\right) - \frac{\Delta G^{\ddagger}}{RT}$$

$$\longrightarrow \ln\left(\frac{k}{T}\right) = -\frac{\Delta G^{\ddagger}}{RT} + \ln\left(\frac{k'}{h}\right)$$

Recall that $\Delta G^{\ddagger} = \Delta H^{\ddagger} - T\Delta S^{\ddagger}$ and so the Eyring equation can now be rewritten in terms of enthalpy and entropy of activation.

$$\ln\left(\frac{k}{T}\right) = -\frac{\Delta H^{\ddagger}}{RT} + \frac{\Delta S^{\ddagger}}{R} + \ln\left(\frac{k'}{h}\right)$$

If we now plot this equation, we see that $-\Delta H^{\ddagger}/RT$ is the slow while $\Delta S^{\ddagger}+\ln(k'/h)$ is the y-intercept.
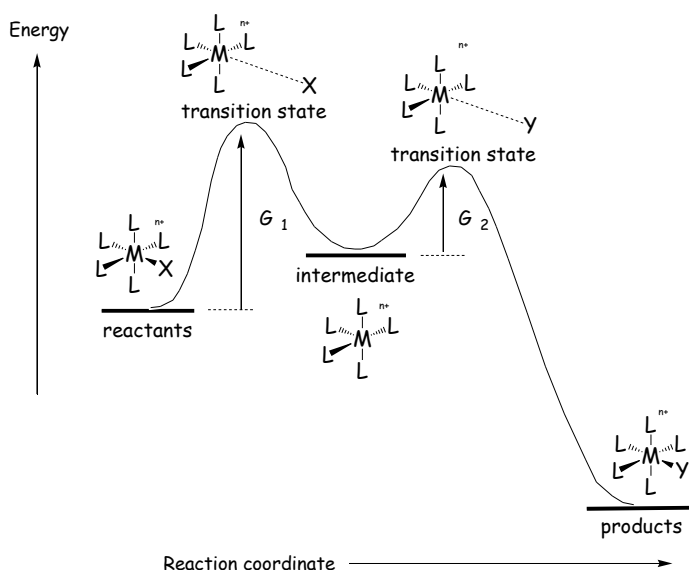
The reaction coordinate diagram on the preceding page represents a concerted reaction, proceeding via a transition state (like an S_N2 reaction). The energy diagram to the left represents a two-step reaction with an intermediate. Let's now look in more detail at the difference in reaction progression between an associative and a dissociative mechanism.

In a dissociative process, the first step is the rate determining step while in an associative process, the second step is rate determining.

A dissociative process

An associative process
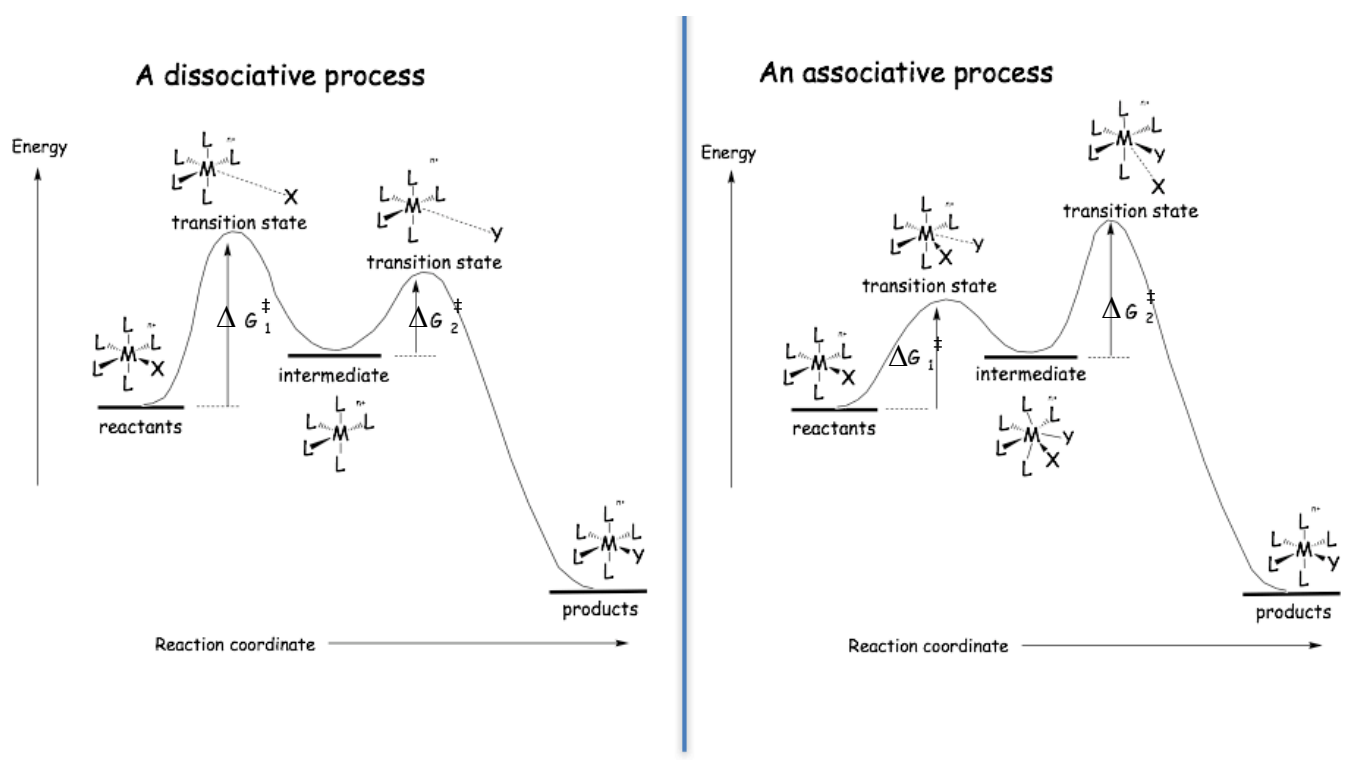
Let's look at some examples and return to water exchange on aqua metal ions.

	Metal ion	d^n config	Mechanism	$\Delta H^{\ddagger}$ kJ mol^{-1}	$\Delta S^{\ddagger}$ J K^{-1} mol^{-1}
increasing e_g occupancy ↓	$[V(H_2O)_6]^{2+}$	$t_{2g}^3 e_g^0$	associative	62	~0
	$[Mn(H_2O)_6]^{2+}$	$t_{2g}^3 e_g^2$	associative	33	+6
increasing t_{2g} occupancy	$[Fe(H_2O)_6]^{2+}$	$t_{2g}^4 e_g^2$	increasingly dissociative	41	+21
	$[Co(H_2O)_6]^{2+}$	$t_{2g}^5 e_g^2$		46	+37
	$[Ni(H_2O)_6]^{2+}$	$t_{2g}^6 e_g^2$		57	+32

From this data we can see that increasing e_g occupancy leads to higher lability (smaller $\Delta H^{\ddagger}$) but doesn't change the mechanism while increasing t_{2g} occupancy correlates with an increase in $\Delta H^{\ddagger}$ and a more positive $\Delta S^{\ddagger}$ and leads to dissociative behaviour.

$\Delta H^{\ddagger}$ correlates with LFSE, which is a measure of the strength of the M-OH$_2$ bond. However, $\Delta H^{\ddagger}$ is of limited use as a mechanistic indicator as all values are positive.

We saw previously that k_{ex} correlates with LFSE. We can now deduce that k_{ex} correlates with $\Delta H^{\ddagger}$. This is entirely expected as, regardless of the mechanism, there will be a bond-breaking event along the reaction coordinate (most endothermic step of the reaction, most impacting the rate).

What about the entropy of activation? $\Delta S^{\ddagger}$ to a certain extent correlates with the mechanistic trend BUT this value is prone to large errors based on the mathematical extrapolation to infinite temperature.

Is there another parameter available that we can use as an indicator of the mechanistic pathway? The answer is YES and it is the activation volume, $\Delta V^{\ddagger}$. Let's now consider the two possible pathways again.
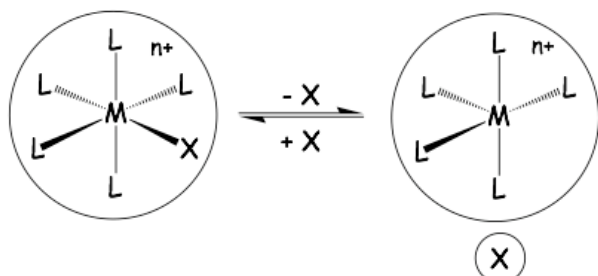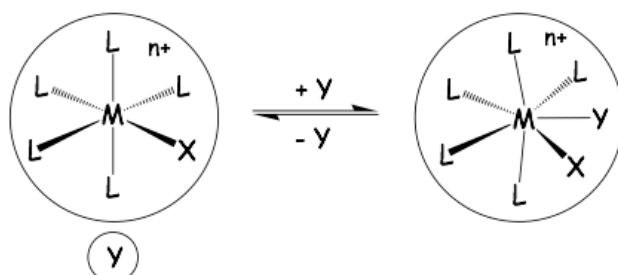
The dissociative process with have a positive $\Delta V^{\ddagger}$. The increase in $\Delta V^{\ddagger}$ corresponds to the volume of free X. The associative process with have a negative $\Delta V^{\ddagger}$. The decrease in $\Delta V^{\ddagger}$ corresponds to the volume of free Y.

How do we measure $\Delta V^{\ddagger}$?
From the pressure dependence of the reaction rate:

$$\frac{d (\ln k)}{dP} = \frac{-\Delta V^{\ddagger}}{RT}$$

A plot of ln k vs P will provide a slope of $-\Delta V^{\ddagger}/RT$. A positive slope (so $\Delta V^{\ddagger}$ is negative) represents an associative mechanism while a negative slope (so $\Delta V^{\ddagger}$ is positive) represents a dissociative mechanism. No change in slope represents a concerted mechanism and an interchange (I) mechanism.

We can now appreciate why various mechanisms would have such rate/pressure dependencies.
A **dissociative** process involves the expulsion of the leaving ligand X (expansive) so would be expected to be retarded by applying pressure: negative slope - positive activation volume.

An **associative** process involves the take up of Y (compressive) so would be expected to be accelerated by applying pressure: positive slope - negative activation volume.

Let's go back to the previous example:

	Metal ion	d^n config	Mechanism	$\Delta H^{\ddagger}$ kJ mol^{-1}	$\Delta S^{\ddagger}$ J K^{-1} mol^{-1}	$\Delta V^{\ddagger}$ cm^3 mol^{-1}
increasing e_g occupancy	$[V(H_2O)_6]^{2+}$	$t_{2g}^3 e_g^0$	associative	62	~0	-4.1
	$[Mn(H_2O)_6]^{2+}$	$t_{2g}^3 e_g^2$	associative	33	+6	-5.4
increasing t_{2g} occupancy	$[Fe(H_2O)_6]^{2+}$	$t_{2g}^4 e_g^2$	increasingly dissociative	41	+21	+3.7
	$[Co(H_2O)_6]^{2+}$	$t_{2g}^5 e_g^2$		46	+37	+6.1
	$[Ni(H_2O)_6]^{2+}$	$t_{2g}^6 e_g^2$		57	+32	+7.2

We can now see that $\Delta V^{\ddagger}$ is a good indicator of the mechanism.

Increase in e_g occupancy **lowers** $\Delta H^{\ddagger}$ but doesn't change the mechanism, where it remains **associative** while an increase in t_{2g} occupancy **increases** $\Delta H^{\ddagger}$ AND gives positive values for $\Delta V^{\ddagger}$, thereby altering the mechanism to one that becomes more **dissociative**.

We can understand these trends from an MO perspective. Increasing e_g occupancy weakens (lengthens) the resident $M\text{-}OH_2$ bonds – decreasing LFSE and lowering $\Delta H^{\ddagger}$ – and increases the rate of exchange. However, increasing t_{2g} occupancy will repel the electrons on the entering ligand Y - facilitating the **dissociative** pathway. As the metal centre gets smaller, the reaction becomes more dissociative. Jahn-Teller distortion will also favour a dissociative mechanism of the first two water molecules.